Electronic Supplementary Material (ESI) for Dalton Transactions.

Supporting Information

for

Biologically active $[Pd_2L_4]^{4+}$ quadruply stranded helicates: cytotoxicity and stability

Samantha M. McNeill,[a] Dan Preston,[b] James E. M Lewis,[b] Anja Robert,[a] Katrin Knerr-Rupp,[a] Danyon O'Neill Graham,[a] James R. Wright,[b] Gregory. I. Giles,[a,] and James D. Crowley[b,]**

[a]Department of Pharmacology and Toxicology, University of Otago, PO Box 56, Dunedin, New Zealand.

[b]Department of Chemistry, University of Otago, PO Box 56, Dunedin, New Zealand;
Fax: +64 3 479 7906; Tel: +64 3 479 7731.

*Corresponding Authors:

jcrowley@chemistry.otago.ac.nz

gregory.giles@otago.ac.nz

Contents

1 Synthetic Experimental Procedures

1.1 General

Unless otherwise stated, all reagents were purchased from commercial sources and used without further purification. Solvents were laboratory reagent grade. Petroleum ether refers to the fraction of petroleum ether boiling in the range 40-60 °C. ^{1}H and ^{13}C NMR spectra were recorded on either a 400 MHz Varian 400 MR or Varian 500 MHz VNMRS spectrometer. Chemical shifts are reported in parts per million and referenced to residual solvent peaks ($CDCl_3$: ^{1}H δ 7.26 ppm, ^{13}C δ 77.16 ppm; CD_3CN: ^{1}H δ 1.94, ^{13}C δ 1.32, 118.26 ppm, d_6-DMSO: ^{1}H δ 2.50 ppm; ^{13}C δ 39.52 ppm). Coupling constants (*J*) are reported in Hertz (Hz). Standard abbreviations indicating multiplicity were used as follows: m = multiplet, q = quartet, t = triplet, dt = double triplet, d = doublet, dd = double doublet, s = singlet, br = broad. IR spectra were recorded on a Bruker ALPHA FT-IR spectrometer with an attached ALPHA-P measurement module. Microanalyses were performed at the Campbell Microanalytical Laboratory at the University of Otago. Electrospray mass spectra (ESMS) were collected on a Bruker micro-TOF-Q spectrometer.

The ligands **tripy**, **bntrz**, **hextrz**, and their respective $[Pd_2\mathbf{L}_4](BF_4)_4$ cages were synthesised as previously reported,[1] as was 1-chloro-2-(2-methoxyethoxy)ethane,[2] dibromobis(benzimidazolin-2-ylidene)dipalladium(II)[3] and **monobntrz**.[1a]

1.2 The use of models complexes for ^{13}C carbene probes

Ethynylpyridine, **monobntrz**, **monohextrz** and **monopegtrz** were used as proxies for **tripy**, **bntrz**, **hextrz**, **pegtrz** in the NHC ^{13}C NMR carbene probes to assess electronic ligand strength rather than the actual ligands due to problems generating pure disubstituted product for the triazole-based ligands (**bntrz**, **hextrz**). In solution an equilibrium mixture of product, monosubstituted compound and dibromobis(benzimidazolin-2-ylidene)dipalladium(II)[3] was evident in the attempted synthesis of $[Pd_2(NHC)_2(bntrz)Br_4]$ (see 1.12), despite crystallisation of the desired product (see Figure 4.6). Additionally, the NMR spectra were complicated by the presence of rotamers. The tripyridyl probe was successfully synthesised, and although it crystallised as the trisubstituted product (Figure 4.5), NMR and mass spectral evidence confirm the clean formation of the disubstituted product in solution. Importantly, the ^{13}C chemical shift of the carbene carbon used to probe the electronic donor strength of the ligands was consistent between the ethynylpyridyl model and the complex containing **tripy** (158.7 versus 158.8 ppm); Suggesting that the model ligands provide a good estimation of the electronic strength of the actual ligands (see 1.11).

1.3 ^{1}H DOSY NMR DATA

^{1}H DOSYNMR spectroscopy was used to calculate the diffusion coefficients of two Pd_2L_4 helicates in 3:2 d_6-DMSO/D_2O, (500 MHz, 298K); the diffusion coefficients of $[Pd_2(\mathbf{pegtrz})_4](BF_4)_4$ and $[Pd_2(\mathbf{hextrz})_4](BF_4)_4$ were 0.63×10^{-10} m^2s^{-1} and 0.74×10^{-10} m^2s^{-1} respectively.

Note: CAUTION, WHILE NO PROBLEMS WERE ENCOUNTERED IN THE COURSE OF THIS WORK, AZIDES ARE POTENTIALLY EXPLOSIVE

1.4 Synthesis of pegtrz (1,3-bis(1-(2-(2-methoxyethoxy)ethyl)-1H-1,2,3-triazol-4-yl)benzene)

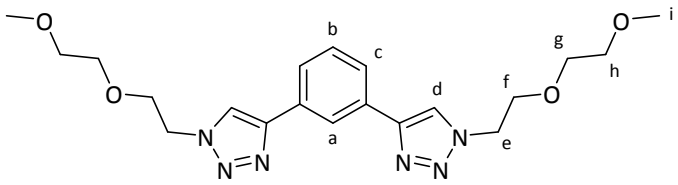

To a stirred solution of 1-chloro-2-(2-methoxyethoxy)ethane[2] (500 mg, 3.61 mmol, 2.1 eq.) in DMF/H_2O (4:1, 10 mL) was added NaN_3 (246 mg, 3.78 mmol, 2.2 eq.) and the solution was microwaved at 125 °C at 250 W for 3.5 hours. After adding L-ascorbic acid (299 mg, 1.72 mmol, 1 eq.), $CuSO_4 \cdot 5H_2O$ (214 mg, 0.86 mmol, 0.5 eq.) and 1,3-diethynylbenzene (217 mg, 1.72 mmol, 1 eq.), the solution was stirred at room temperature overnight. The reaction mixture was poured into a 0.1 M EDTA/NH_4OH aqueous solution (50 mL) and stirred vigorously for 30 minutes. The suspension was extracted into DCM (2 x 100 mL), and the combined organic layers were dried with Na_2SO_4, filtered, and the solvent removed *in vacuo*. The residue was purified via column chromatography on silica (1:1 DCM/Petroleum ether to DCM to 1:5 acetone/DCM) to give the product as a green oil (515 mg, 1.24 mmol, 72%). ^{1}H NMR ($CDCl_3$, 298 K, 400 MHz) δ: 8.36 (t, 1H, J = 1.6 Hz, H_a), 8.27 (s, 2H, H_d), 7.84 (dd, 2H, J = 7.3 Hz, 1.7 Hz, H_c), 7.53 (t, 1H, J = 7.8 Hz, H_b), 4.58 (t, 4H, J = 5.1 Hz, H_e), 3.92 (t, 4H, J = 5.2 Hz, H_f), 3.62-3.60 (m, 4H, H_g), 3.49-3.47 (m, 4H, H_h), 3.30 (s, 6H, H_i). ^{13}C NMR ($CDCl_3$, 298 K, 100 MHz) δ: 146.7, 131.8, 129.5 (C_b), 124.8 (C_c), 122.2 (C_a), 121.5 (C_d), 71.5 (C_h), 70.0 (C_g), 68.9 (C_f), 58.0 (C_i), 50.1 (C_e). HR ESI-MS (CH_3CN) *m/z* = 417.2218 [**M** + H]$^+$ (calc. for $C_{20}H_{29}N_6O_4$, 417.2245), *m/z* = 439.2046 [**M** + Na]$^+$ (calc. for $C_{20}H_{28}N_6NaO_4$, 439.2064), *m/z* = 855.4161 [2**M** + Na]$^+$ (calc. for $C_{40}H_{56}N_{12}NaO_8$, 855.4236). Anal. calcd. for $C_{20}H_{28}N_6O_4$: C, 57.68; H, 6.78; N, 20.18%; Found: C, 57.64; H, 6.91; N, 20.17%. IR: *v* (cm^{-1}) 3120, 3092, 3063, 2954, 2927, 2869, 2855, 1463, 1077.

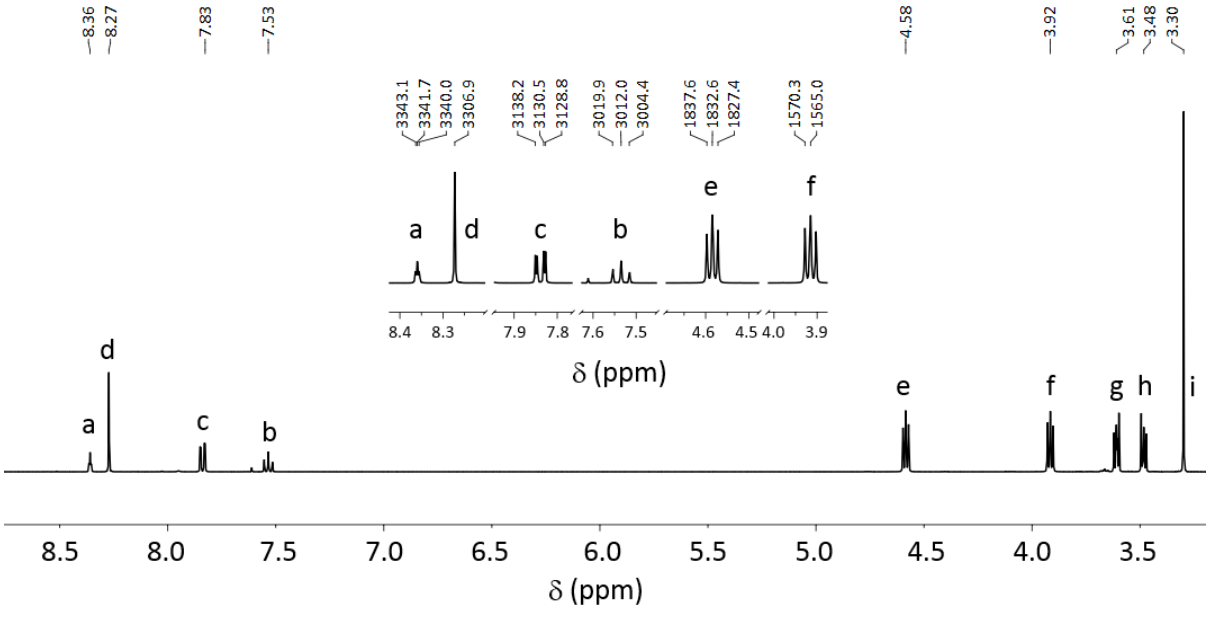

Figure 1.1 Partial ^{1}H NMR spectrum (298 K, 400 MHz, CD_3CN) of **pegtrz**.

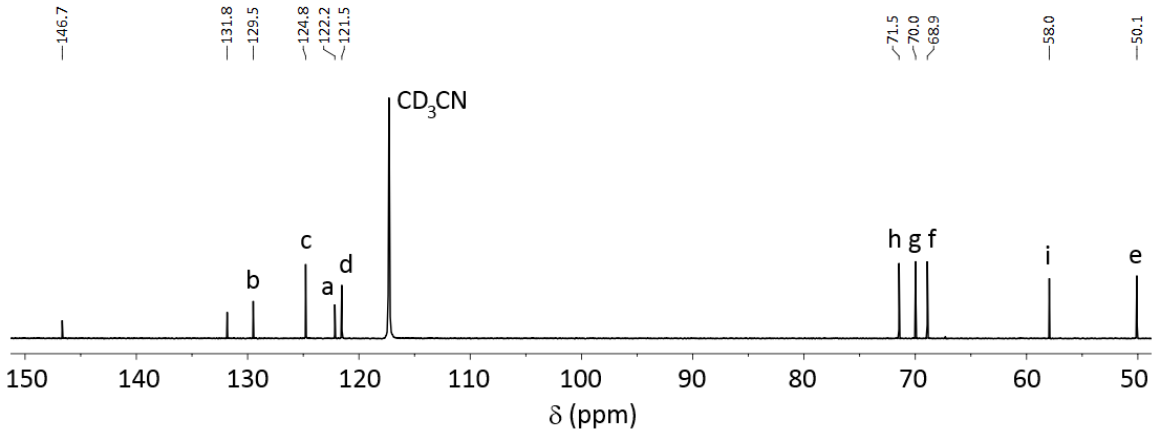

Figure 1.2 Partial ^{13}C NMR spectrum (298 K, 100 MHz, CD_3CN) of **pegtrz**.

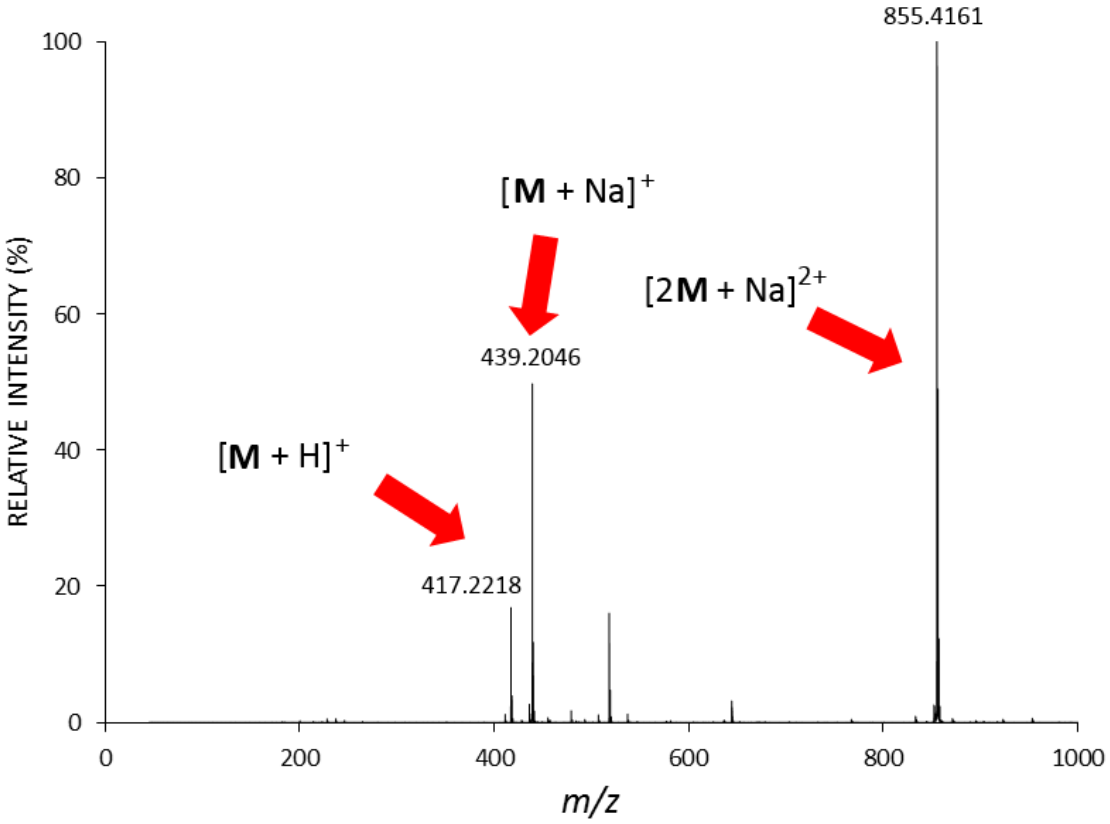

Figure 1.3 HR-ESI Mass spectrum of **pegtrz** (CH_3CN).

1.5 Synthesis of $[Pd_2(pegtrz)_4](BF_4)_4$

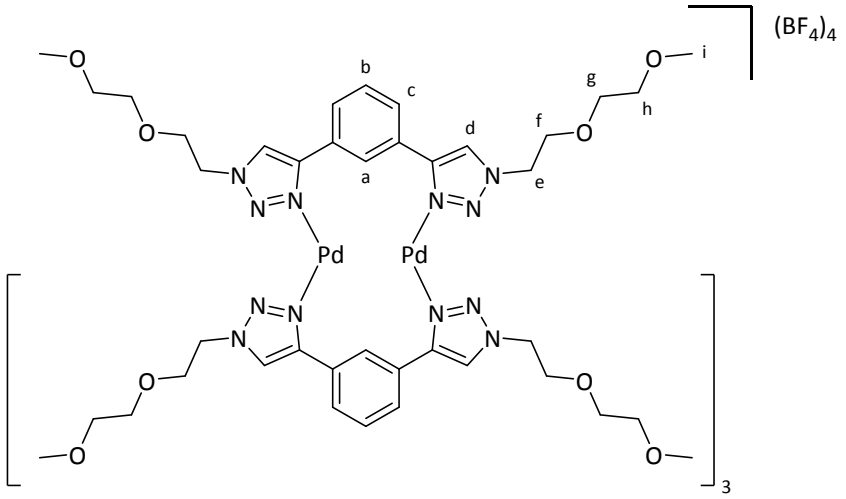

A solution of **pegtrz** (100 mg, 0.24 mmol, 4 eq.) and $[Pd(CH_3CN)_4](BF_4)_2$ (53 mg, 0.12 mmol, 2 eq.) in CD_3CN (0.75 ml) was heated at 75 °C for 3 hours. Addition of diethyl ether (5 mL) brought about formation of a green oil. The solvent was decanted and the sample dried *in vacuo*, giving the product as an oil (115 mg, 0.052 mmol, 86%). ^{1}H NMR ($CDCl_3$, 298 K, 400 MHz) δ: 10.24 (s, 1H , H_a), 8.10 (s, 2H,H_d), 7.48 (t, 1H, J = 8.3 Hz, H_b), 7.36 (dd, 2H, J = 8 Hz, 1.4 Hz, H_c), 4.34 - 4.21 (m, 4H, H_f), 3.71 - 3.66 (m, 2H, H_{e1}), 3.54, 3.44 (m, 10H, H_e, H_g, H_h), 3.30 (s, 6H, H_i). ^{13}C NMR ($CDCl_3$, 298 K, 100 MHz) δ: 146.2, 131.1 (C_b), 130.0 (C_c), 127.0 (C_d), 125.9, 121.6 (C_a), 71.4 (C_g or C_h), 69.9 (C_g or C_h), 67.4 (C_f), 58.0 (C_i), 52.4 (C_e). DOSY diffusion coefficient (x 10^{-10} m^2 s^{-1}): 0.63. HR ESI-MS (CH_3CN) m/z = 469.6712 [**M** – $(BF_4)_4$]$^{4+}$ (calc. for $C_{80}H_{112}N_{24}O_{16}$, 469.6693), m/z = 655.2315 [**M** – $(BF_4)3$]$^{3+}$ (calc. for $C_{80}H_{112}BF_4N_{24}O_{16}$, 655.2271), m/z = 1026.3470 [**M** – $(BF_4)_2$]$^{2+}$ (calc. for $C_{80}H_{112}B_2F_8N_{24}O_{16}$, 1026.3428). Anal. calcd. for $C_{80}H_{112}B_4F_{16}N_{24}O_{16}Pd_2$: C, 43.17; H, 5.07; N, 15.10%; Found: C, 42.87; H, 5.24; N, 14.82%. IR: ν (cm^{-1}) 3150, 2883, 2821, 1566, 1454, 1367, 1353, 1095, 1049.

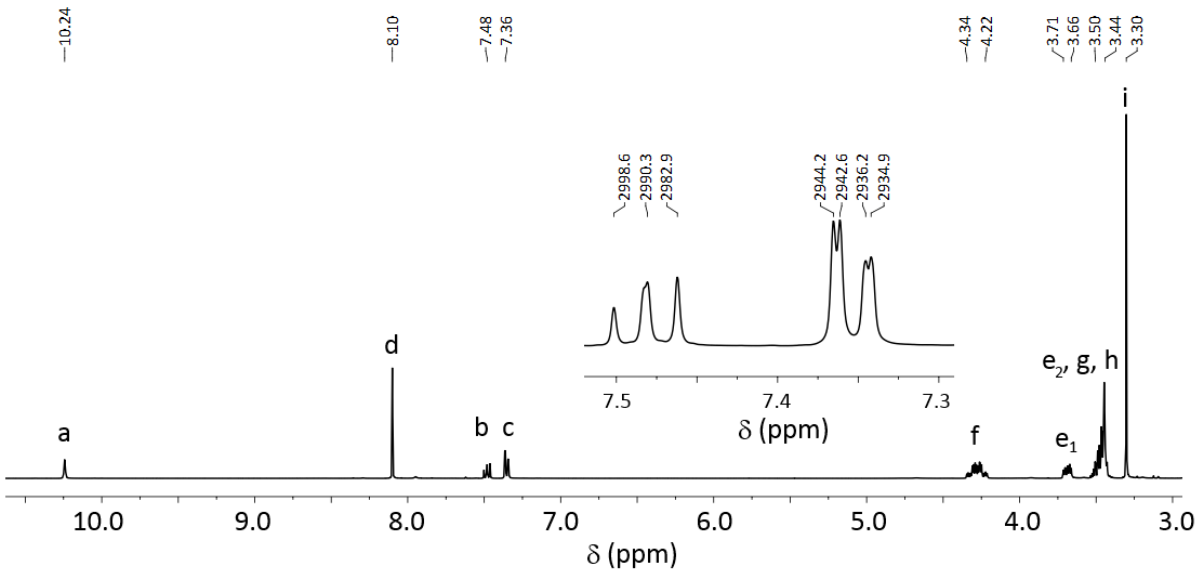

Figure 1.4 Partial ^{1}H NMR spectrum (298 K, 400 MHz, CD_3CN) of $[Pd_2(\mathbf{pegtrz})_4](BF_4)_4$.

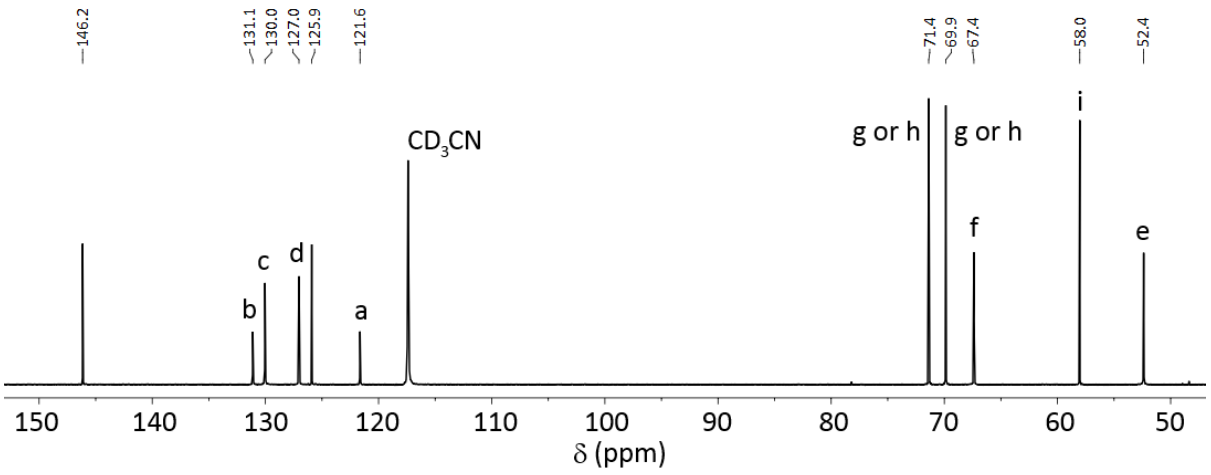

Figure 1.5 Partial ^{13}C NMR spectrum (298 K, 100 MHz, CD_3CN) of $[Pd_2(\mathbf{pegtrz})_4](BF_4)_4$.

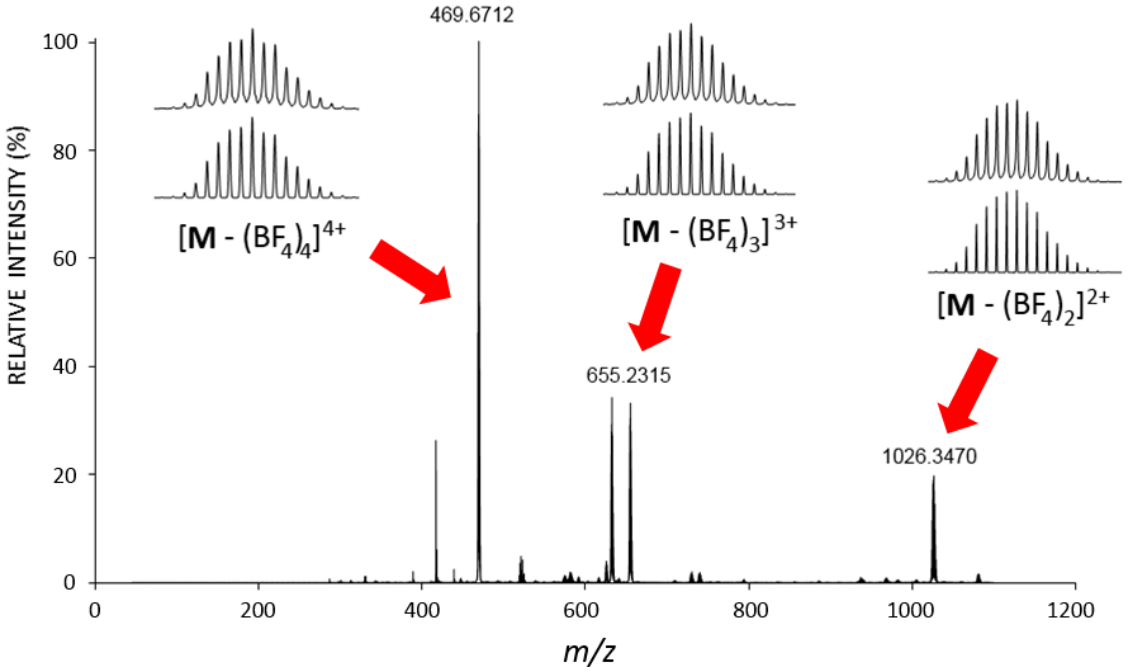

Figure 1.6 HR-ESI Mass spectrum of $[Pd_2(\mathbf{pegtrz})_4](BF_4)_4$ (CH_3CN).

1.6 Synthesis of monohextrz

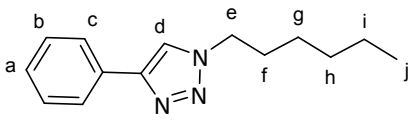

A solution of sodium azide (70 mg, 1.07 mmol, 1.1 eq.), sodium iodide (73 mg, 0.49 mmol, 0.5 eq.) and 1-bromohexane (170 mg, 1.03 mmol, 1.05 eq.) in 4:1 DMF/H_2O (15 mL) was microwaved at 125 °C at 250 W for 45 minutes. After cooling to room temperature, ethynylbenzene (107 µL, 100 mg, 0.98 mmol, 1 eq.), sodium ascorbate (194 mg, 0.98 mmol, 1 eq.) and $CuSO_4 \cdot 5H_2O$ (244 mg, 0.98 mmol, 1 eq.) were added and the resulting suspension was stirred at room temperature for 20 hours, before adding 0.1 M EDTA/NH_4OH aqueous solution (20 mL) and stirring vigorously for 30 minutes. The organic extract was then washed with 0.1 M EDTA/NH_4OH aqueous solution (40 mL), water (40 mL) and brine (40 mL) then dried over $MgSO_4$, before filtration and removal of the solvent under vacuum. The resulting residue was then purified by column chromatography on silica (DCM) to give the product as a colourless solid (158 mg, 0.69 mmol, 70%). Mp: 73.9 °C. ^{1}H NMR ($CDCl_3$, 298 K, 400 MHz) δ: 7.84 (2H, d, J = 7.1 Hz, H_c), 7.74 (1H, s, H_d), 7.42 (2H, t, J = 7.6 Hz), 7.33 (1H, t, J = 7.5 Hz H_a), 4.39 (2H, t, J = 8.0 Hz, H_e), 1.95 (2H, q, J = 7.1 Hz, H_f), 1.38-1.31 (6H, m, H_g, H_h, H_i), 0.89 (3H, t, J = 7.0 Hz, H_j). ^{13}C NMR ($CDCl_3$, 298 K, 100 MHz) δ: 147.7, 130.7, 128.8 (C_b), 128.0 (C_a), 125.7 (C_c), 119.3 (C_d), 50.4 (C_e), 31.2 (C_h), 30.3 (C_f), 26.2 (C_g), 22.4 (C_i), 13.9 (C_j). HR ESI-MS (CH_3OH) m/z = 230.1632 [**M** + H]$^+$ (calc. for $C_{14}H_{20}N_3$, 230.1652), m/z = 252.1453 [**M** + Na]$^+$ (calc. for $C_{14}H_{19}N_3Na$, 252.1471). Anal. calcd. for $C_{14}H_{19}N_3 \cdot 0.1H_2O$: C, 72.75; H, 8.37; N, 18.18%; Found: C, 72.83; H, 8.50; N, 18.58%. IR: ν (cm^{-1}) 3120, 3063, 2955, 2927, 2869, 1463, 1440, 1216, 1077.

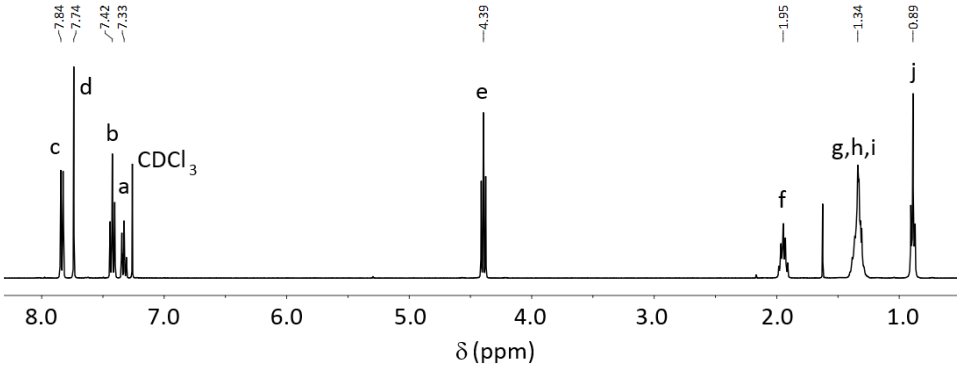

Figure 1.7 Partial ^{1}H NMR spectrum (298 K, 400 MHz, $CDCl_3$) of **monohextrz**.

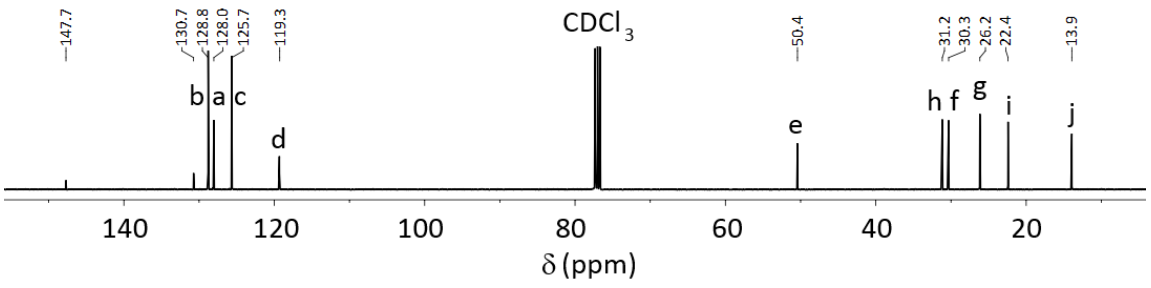

Figure 1.8 Partial ^{13}C NMR spectrum (298 K, 100 MHz, $CDCl_3$) of **monohextrz**.

1.7 Synthesis of monopegtrz

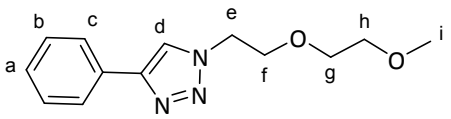

A solution of sodium azide (70 mg, 1.07 mmol, 1.1 eq.), sodium iodide (73 mg, 0.49 mmol, 0.5 eq.) and 1-chloro-2-(2-methoxyethoxy)ethane (142 mg, 1.03 mmol, 1.05 eq.) in 4:1 DMF/H_2O (15 mL) was microwaved at 125 °C at 250 W for 3 hours. After cooling to room temperature, ethynylbenzene (107 µL, 100 mg, 0.98 mmol, 1 eq.), sodium ascorbate (194 mg, 0.98 mmol, 1 eq.) and $CuSO_4 \cdot 5H_2O$ (244 mg, 0.98 mmol, 1 eq.) were added and the resulting suspension was stirred at room temperature for 20 hours, before adding 0.1 M EDTA/NH_4OH aqueous solution (20 mL) and stirring vigorously for 30 minutes. The organic extract was then washed with 0.1 M EDTA/NH_4OH aqueous solution (40 mL), water (40 mL) and brine (40 mL) then dried over $MgSO_4$, before filtration and removal of the solvent under vacuum. The resulting residue was then purified by column chromatography on silica (DCM then 3:2 DCM/acetone) to give the product as a colourless oil (163 mg, 0.66 mmol, 67%). ^{1}H NMR ($CDCl_3$, 298 K, 400 MHz) δ: 8.00 (1H, s, H_d), 7.85 (2H, d, J = 8.0 Hz, H_c), 7.42 (2H, t, J = 7.6 Hz, H_b), 7.32 (1H, t, J = 7.4 Hz, H_a), 4.60 (2H, t, J = 5.1 Hz, H_e), 3.91 (2H, t, J = 5.0 Hz, H_f), 3.63-3.61 (2H, m, H_g), 3.53-3.51 (2H, m, H_h), 3.37 (3H, s, H_i). ^{13}C NMR ($CDCl_3$, 298 K, 100 MHz) δ: 147.7, 130.8, 128.8 (C_b), 128.0 (C_a), 125.6 (C_c), 120.9 (C_d), 71.7 (C_h), 70.5 (C_g), 69.5 (C_f), 59.0 (C_i), 50.3 (C_e). HR ESI-MS (CH_3OH) *m/z* = 248.1371 [**M** + H]$^+$ (calc. for $C_{13}H_{18}N_3O_2$, 248.1394), *m/z* = 270.1215 [**M** + Na]$^+$ (calc. for $C_{13}H_{17}N_3NaO_2$, 270.1213). Anal. calcd. for $C_{13}H_{17}N_3O_2 \cdot 0.1H_2O$: C, 62.68; H, 6.96; N, 16.87%; Found: C, 62.50; H, 7.01; N, 17.16%. IR: ν (cm^{-1}) 3126, 3095, 2953, 2925, 2870, 1464, 1104, 1077, 1048.

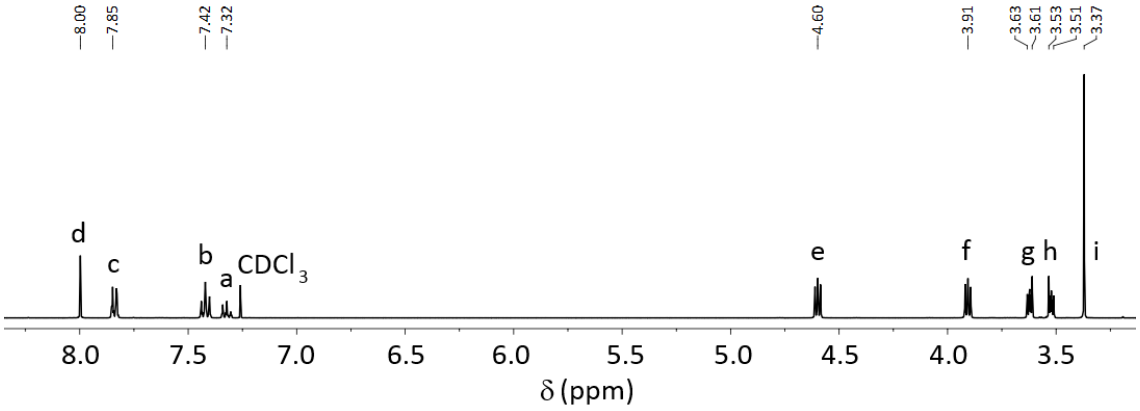

Figure 1.9 Partial ^{1}H NMR spectrum (298 K, 400 MHz, $CDCl_3$) of **monopegtrz**.

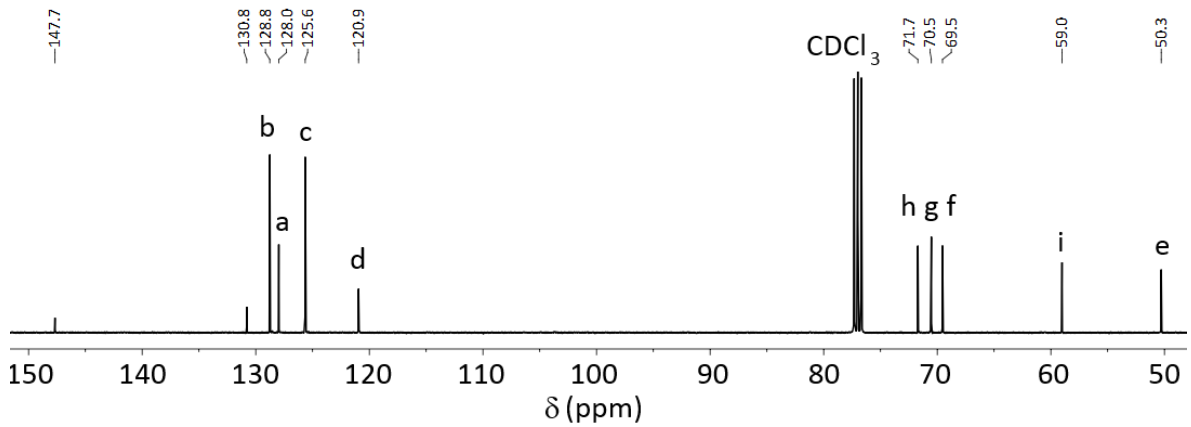

Figure 1.10 Partial ^{13}C NMR spectrum (298 K, 100 MHz, $CDCl_3$) of **monopegtrz**.

1.8 Synthesis of [Pd(NHC)(monobntrz)Br_2]

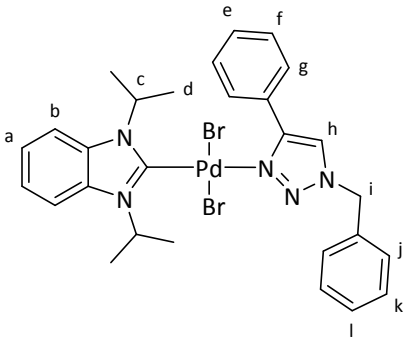

A solution of **monobntrz**[1a] (9.9 mg, 0.042 mmol, 1 eq.) and dibromorobis(benzimidazolin-2-ylidene)dipalladium(II)[3] (20 mg, 0.021 mmol, 0.5 eq.) in $CDCl_3$ (0.75 mL) was sonicated for 30 seconds. A yellow crystalline material was obtained through vapour diffusion of diethyl ether into $CDCl_3$ (21 mg, 0.030 mmol, 71%). Mp: >230 °C. ^1H NMR ($CDCl_3$, 298 K, 400 MHz) δ: 8.20 (2H, d, J = 6.7 Hz, H_g), 7.56-7.50 (6H, m, H_b, H_e, H_f, H_h), 7.43-7.36 (5H, m, H_j, H_k, H_l), 7.18 (2H, dd, J = 6.2 Hz, 3.1 Hz, H_a), 6.30 (2H, sept, J = 7.0 Hz, H_c), 5.64 (s, 2H, H_i), 1.73 (12H, d, J = 7.0 Hz, H_d). ^{13}C NMR ($CDCl_3$, 298 K, 100 MHz) δ: 161.3 (carbene), 149.3, 133.6, 133.1, 129.6 (C_g), 129.5 (C_k), 129.4, 129.4, 129.3, 128.8 (C_j), 128.5 (C_f), 122.3 (C_h), 122.2 (C_a), 112.7 (C_b), 55.5 (C_i), 54.5 (C_c), 20.7 (C_d). HR ESI-MS ($CDCl_3$/MeOH) *m/z* = 725.9795 [**M** + Na]$^+$ (calc. for $C_{28}H_{31}Br_2N_5NaPd$, 725.9865). Anal. calcd. for $C_{28}H_{31}Br_2N_5Pd{\cdot}0.4CDCl_3$: C, 45.28; H, 4.23; N, 9.30%; Found: C, 45.18; H, 4.25; N, 9.19%. IR: ν (cm^{-1}) 2976, 1407, 1366, 1315, 1143, 1092.

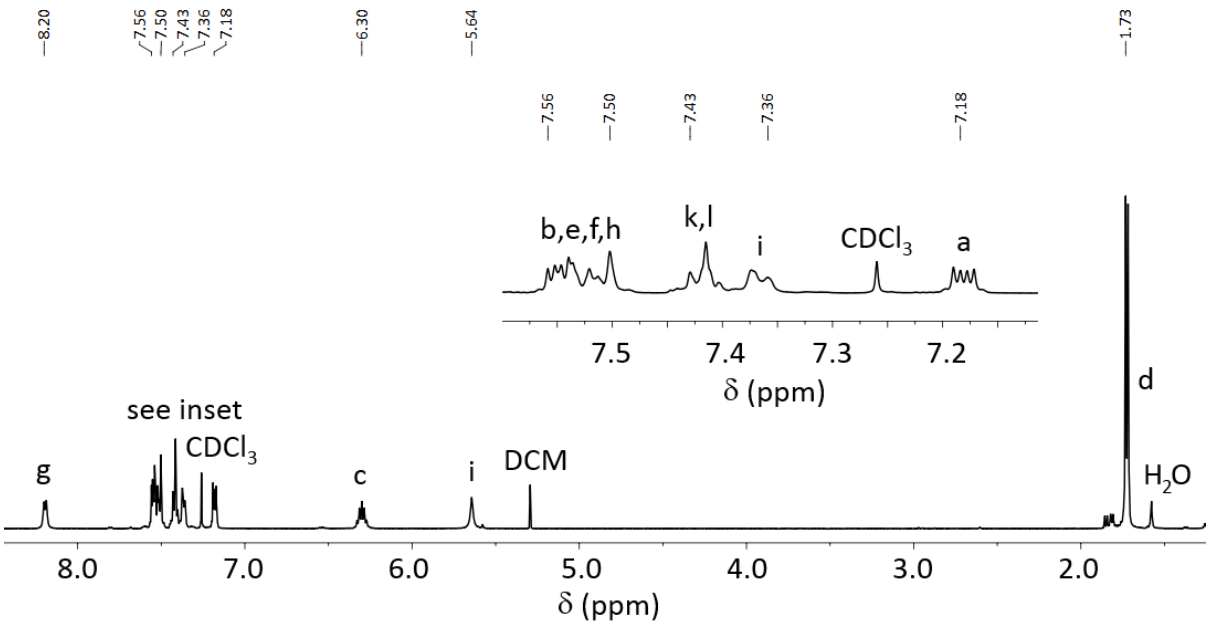

Figure 1.11 Partial ^{1}H NMR spectrum (298 K, 400 MHz, $CDCl_3$) of [Pd(NHC)(**bntrz**)Br_2].

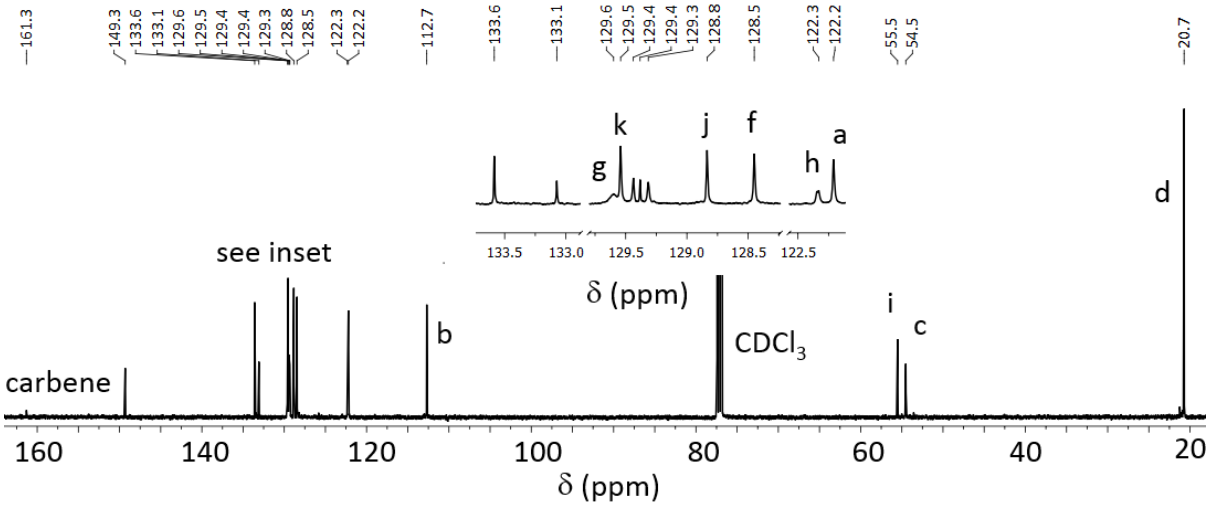

Figure 1.12 Partial ^{13}C NMR spectrum (298 K, 100 MHz, $CDCl_3$) of [Pd(NHC)(**bntrz**)Br_2].

1.9 Synthesis of [Pd(NHC)(monohextrz)Br_2]

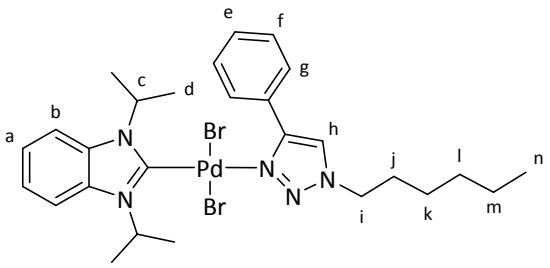

A solution of **monohextrz** (9.6 mg, 0.042 mmol, 1 eq.) and dibromobis(benzimidazolin-2-ylidene)dipalladium(II)[3] (20 mg, 0.021 mmol, 0.5 eq.) in $CDCl_3$ (0.75 mL) was sonicated for 30 seconds. Vapour diffusion of diethyl ether into $CDCl_3$ gave yellow X-ray quality crystals (22.4 mg, 0.032 mmol 76%). Mp: >230 °C. ^{1}H NMR ($CDCl_3$, 298 K, 400 MHz) δ: 8.24 (2H, d, J = 7.1 Hz, H_g), 7.69 (1H, s, H_h), 7.58-7.51 (5H, m, H_b, H_e, H_f), 7.17 (2H, dd, J = 3.1 Hz, 6.2 Hz), 6.28 (2H, quin, J = 6.4 Hz), 4.44 (2H, t, J = 7.1 Hz), 2.00 (2H, t, J = 7.5 Hz H_j), 1.72 (12H, d, J =7.0 Hz), 1.43-1.34 (6H, m, H_k, H_l, H_m), 0.91 (3H, t, J = 7.0 Hz, H_n). ^{13}C NMR ($CDCl_3$, 298 K, 100 MHz) δ: 161.5 (carbene), 148.9, 133.6, 129.6 (H_g), 129.6, 129.3 (C_e), 128.5 (C_f), 54.5 (C_c), 51.9 (C_i), 31.2 (C_l or C_m), 30.2 (C_j), 26.3 (C_k), 22.5 (C_l or C_m), 20.7 (C_d), 14.1 (C_n). HR ESI-MS ($CDCl_3$/MeOH) m/z = 618.1224 [**M** – Br]$^+$ (calc. for $C_{26}H_{35}BrN_5O_2Pd$, 618.1259), m/z = 720.0295 [**M** + Na]$^+$ (calc. for $C_{26}H_{35}Br_2N_5NaO_2Pd$, 720.0343). Anal. calcd. for $C_{27}H_{37}Br_2N_5Pd$: C, 47.47; H, 5.24; N, 9.96%; Found: C, 46.39; H, 5.24; N, 9.96%. IR: ν (cm^{-1}) 3096, 2979, 2932, 2856, 1423, 1409, 1316, 1144, 1092.

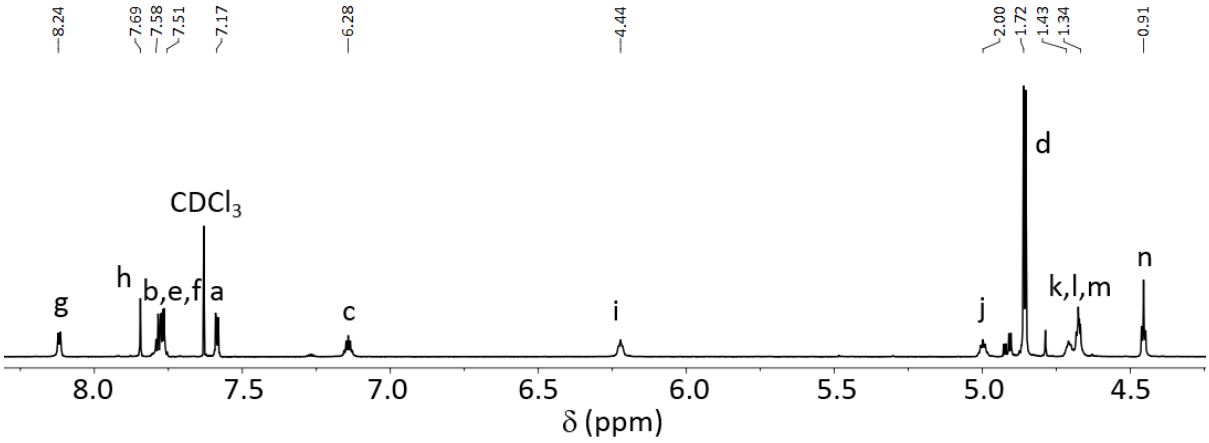

Figure 1.13 Partial ^{1}H NMR spectrum (298 K, 400 MHz, $CDCl_3$) of [Pd(NHC)(**hextrz**)Br_2].

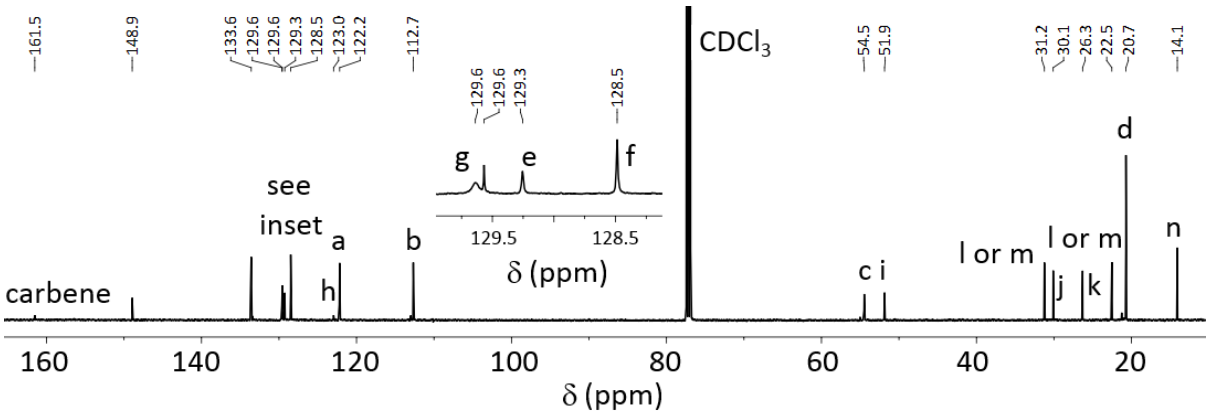

Figure 1.14 Partial ^{13}C NMR spectrum (298 K, 100 MHz, $CDCl_3$) of [Pd(NHC)(**hextrz**)Br_2].

1.10 Synthesis of [Pd(NHC)(monopegtrz)Br_2]

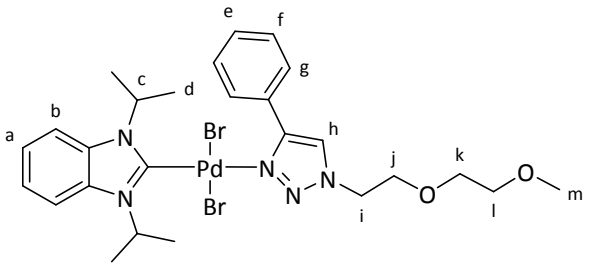

A solution of **monopegtrz** (10.4 mg, 0.042 mmol, 1 eq.) and dibromobis(benzimidazolin-2-ylidene)dipalladium(II)[3] (20 mg, 0.021 mmol, 0.5 eq.) in $CDCl_3$ (0.75 mL) was sonicated for 30 seconds. Vapour diffusion of diethyl ether into $CDCl_3$ gave yellow X-ray quality crystals (27.5 mg, 0.038 mmol, 91%). Mp: >230 °C. ^1H NMR ($CDCl_3$, 298 K, 400 MHz) δ: 8.27 (2H, d, J = 7.3 Hz, H_g), 8.02 (1H, s, H_h), 7.59-7.51 (5H, m, H_b, H_e, H_f), 7.18 (2H, dd, J = 3.1 Hz, 6.1 Hz), 6.29 (2H, sept, J = 7.2 Hz, H_c), 4.66 (2H, t, J = 5.4 Hz, H_i), 3.94 (2H, t, J = 4.6 Hz, H_j), 3.65-3.63 (2H, m, H_k), 3.53-3.51 (2H, m, H_l), 3.35 (3H, s, H_m), 1.71 (12H, d, J =7.0 Hz, H_d). ^{13}C NMR ($CDCl_3$, 298 K, 100 MHz) δ: 161.4 (carbene), 148.9, 133.6, 129.7, 129.6 (C_g), 129.2 (C_e), 128.4 (C_f), 124.1 (C_h), 122.2 (C_a), 112.7 (C_b), 71.8 (C_l), 70.7 (C_k), 69.0 (C_j), 59.1 (C_m), 54.5 (C_c), 51.6 (C_i), 20.7 (C_d). HR ESI-MS ($CDCl_3$/MeOH) m/z = 636.0920 [**M** – Br]$^+$ (calc. for $C_{26}H_{35}BrN_5O_2Pd$, 636.1001), m/z = 738.0000 [**M** + Na]$^+$ (calc. for $C_{26}H_{35}Br_2N_5NaO_2Pd$, 738.0076). Anal. calcd. for $C_{26}H_{35}Br_2N_5Pd$: C, 43.63; H, 4.93; N, 9.78; Found: C, 43.49; H, 4.78; N, 9.75. IR: ν (cm^{-1}) 3125, 3098, 3067, 2976, 2918, 2871, 1411, 1365, 1315, 1141, 1115, 1091.

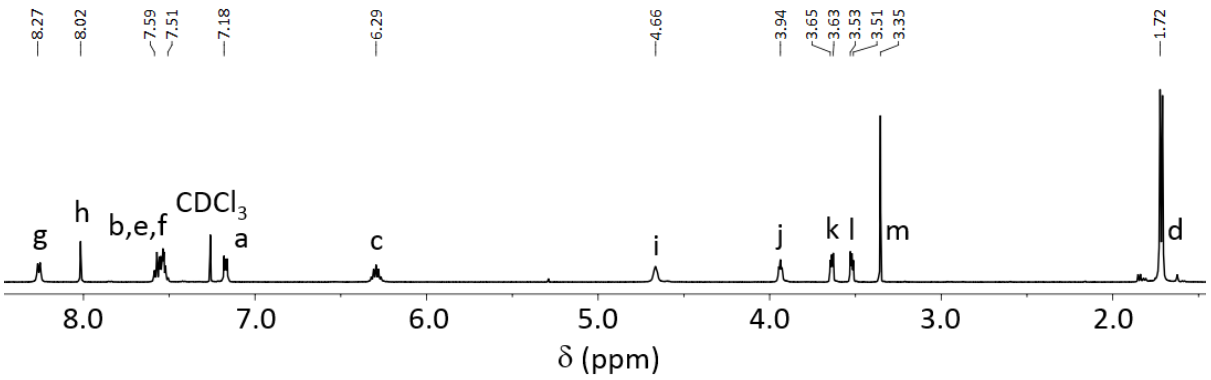

Figure 1.15 Partial ^{1}H NMR spectrum (298 K, 400 MHz, $CDCl_3$) of [Pd(NHC)(**pegtrz**)Br_2].

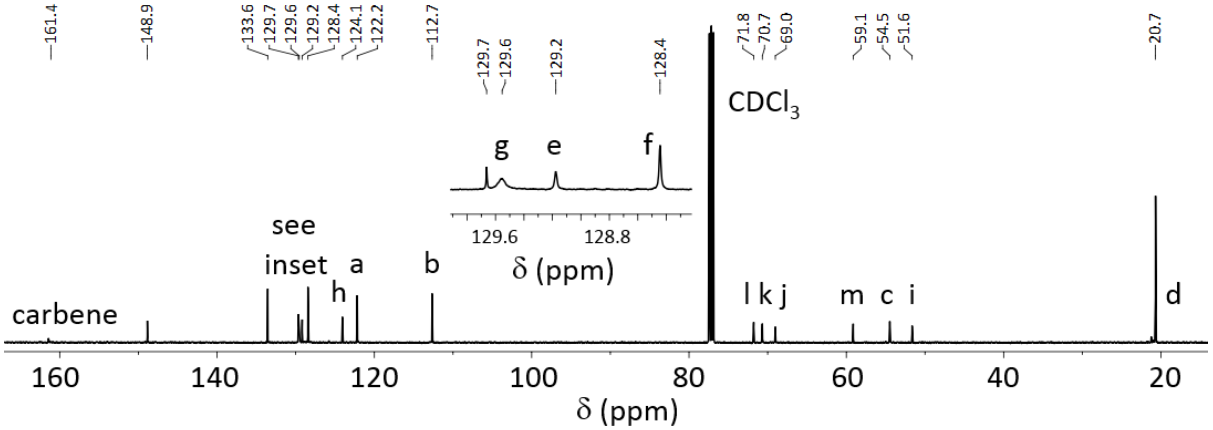

Figure 1.16 Partial ^{13}C NMR spectrum (298 K, 100 MHz, $CDCl_3$) of [Pd(NHC)(**pegtrz**)Br_2].

1.11 Synthesis of [Pd(NHC)(ethynylpyridine)Br_2]

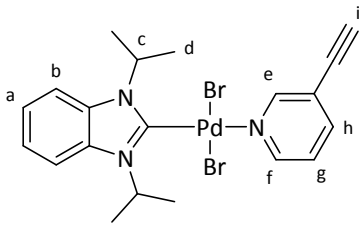

A solution of 3-ethynylpyridine (4.3 mg, 0.042 mmol, 1 eq.) and dibromobis(benzimidazolin-2-ylidene)dipalladium(II)[3] (20 mg, 0.021 mmol, 0.5 eq.) in $CDCl_3$ (0.75 mL) was sonicated for 30 seconds. Vapour diffusion of ether into DCM gave orange block X-Ray quality crystals (22.8 mg, 0.040 mmol, 95%). Mp: decomposes 220 °C. ^{1}H NMR ($CDCl_3$, 298 K, 400 MHz) δ: 9.25 (1H, s, H_e) 9.12 (d, J = 5.5 Hz, H_f), 7.86 (1H, d, J = 7.6 Hz, H_h), 7.59 (2H, dd, J = 2.7 Hz, 6.2 Hz, H_b), 7.33 (1H, dd, J = 6.7 Hz, 7.9 Hz, 6.7 Hz, Hg), 7.22 (2H, dd, J = 3.4 Hz, 5.9 Hz, H_a), 6.31 (2H, sept, J = 7.0 Hz, H_c), 3.29 (1H, s, H_i), 1.80 (12H, d, J = 7.0 Hz, H_d). ^{13}C NMR ($CDCl_3$, 298 K, 100 MHz) δ: 158.7 (carbene), 155.7 (C_e), 152.2 (C_f), 141.0 (C_h), 133.6, 124.0 (C_g), 122.4 (C_a), 120.5, 112.8 (C_b), 82.3 (C_i), 78.9, 54.8 (C_c), 20.7 (C_d). Anal.

calcd. for $C_{20}H_{23}Br_2N_3Pd$: C, 42.02; H, 4.06; N, 7.35; Found: C, 42.23; H, 4.04; N, 7.36. IR: *v* (cm^{-1}) 3208, 2977, 2934, 1407, 1391, 1362, 1314, 1144, 1094. Mass spectral analysis was not successful for this compound.

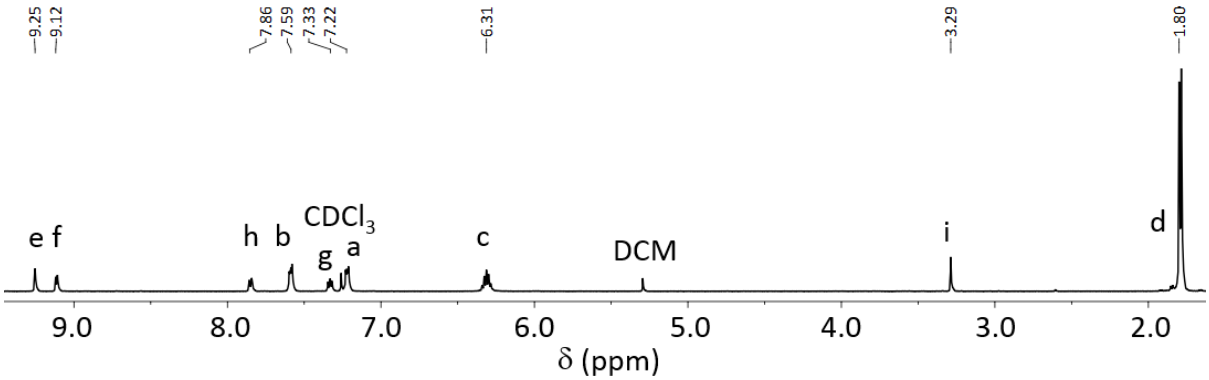

Figure 1.17 Partial ^{1}H NMR spectrum (298 K, 400 MHz, $CDCl_3$) of [Pd(NHC)(ethynylpyridine)Br_2].

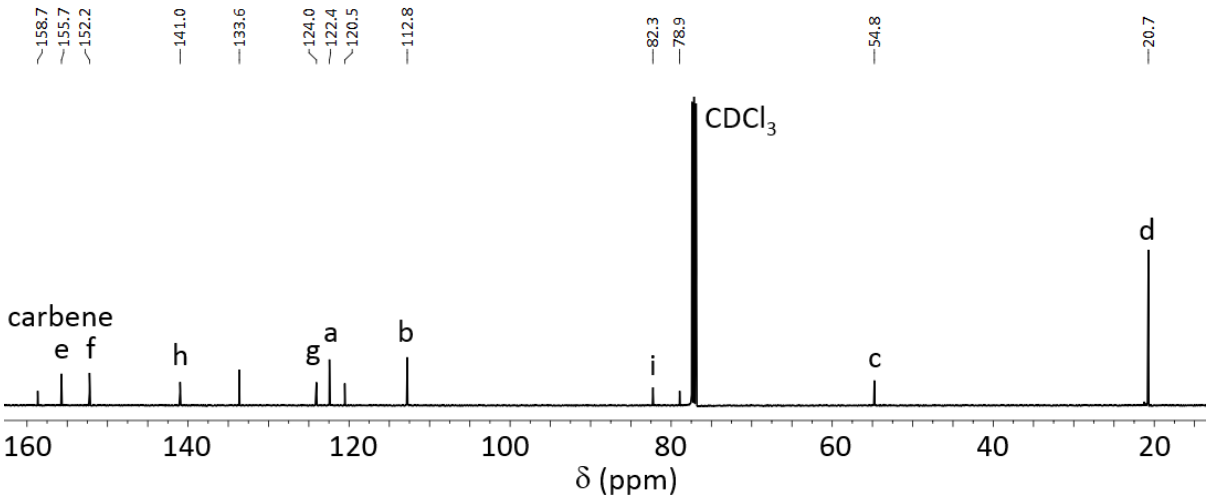

Figure 1.18 Partial ^{13}C NMR spectrum (298 K, 100 MHz, $CDCl_3$) of [Pd(NHC)(ethynylpyridine)Br_2].

1.12 Synthesis of $[Pd_2(NHC)_2(tripy)Br_4]$

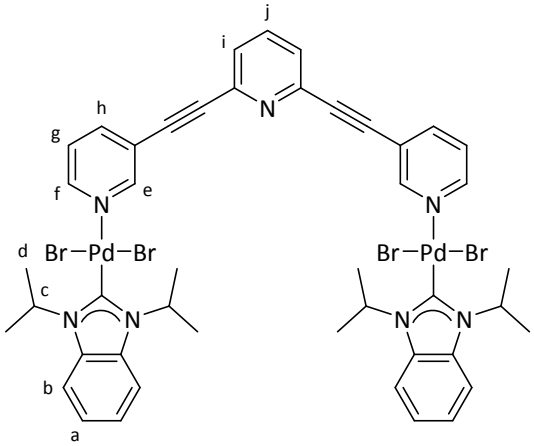

A solution of **tripy** (6.0 mg, 0.021 mmol, 1 eq.) and dibromobis(benzimidazolin-2-ylidene)dipalladium(II)[3] (20 mg, 0.021 mmol, 1 eq.) in $CDCl_3$ (0.75 mL) was sonicated for 30 seconds. Vapour diffusion of diethyl ether gave a yellow crystalline solid (18 mg, 0.015 mmol, 69%) Mp: >230 °C. ^{1}H NMR ($CDCl_3$, 298 K, 400 MHz) δ: 9.38 (2H, s, H_e), 9.14 (2H, d, J = 5.7 Hz, H_f), 7.99 (2H, d, J = 6.5 Hz, H_h), 7.79 (1H, t, J = 7.9 Hz, H_j), 7.61-7.59 (6H, m, H_b & H_i), 7.39 (2H, dd, J = 7.9 Hz, 5.8 Hz, H_g), 7.22 (4H, dd, J = 6.1 Hz, 3.1 Hz H_a), 6.33 (4H, sept, J = 6.6 Hz, H_c), 1.81 (24 H, d, J = 7.0 Hz, H_d). ^{13}C NMR ($CDCl_3$, 298 K, 100 MHz) δ: 158.8 (carbene), 155.6 (C_e), 152.4 (C_f), 143.1, 140.9 (C_h), 137.0 (C_j), 133.7, 127.4 (C_i), 124.2 (C_g), 122.4 (C_a), 120.5, 112.8 (C_b), 92.2, 84.8, 54.8 (C_c), 20.8 (C_d). Anal. calcd. for $C_{45}H_{49}Br_4N_7Pd_2 \cdot 1.5CHCl_3$: C, 39.91; H, 3.64; N, 7.01; Found: C, 39.73; H, 3.60; N, 6.83. ESI-MS ($CDCl_3$/MeOH) m/z = 1241.8717 [**M** + Na]$^+$ (calc. for $C_{45}H_{47}Br_4N_7NaPd_2$, 1241.8571). IR: ν (cm^{-1}) 3275, 2974, 2932, 2225, 1640, 1553, 1473, 1405, 1363, 1312.

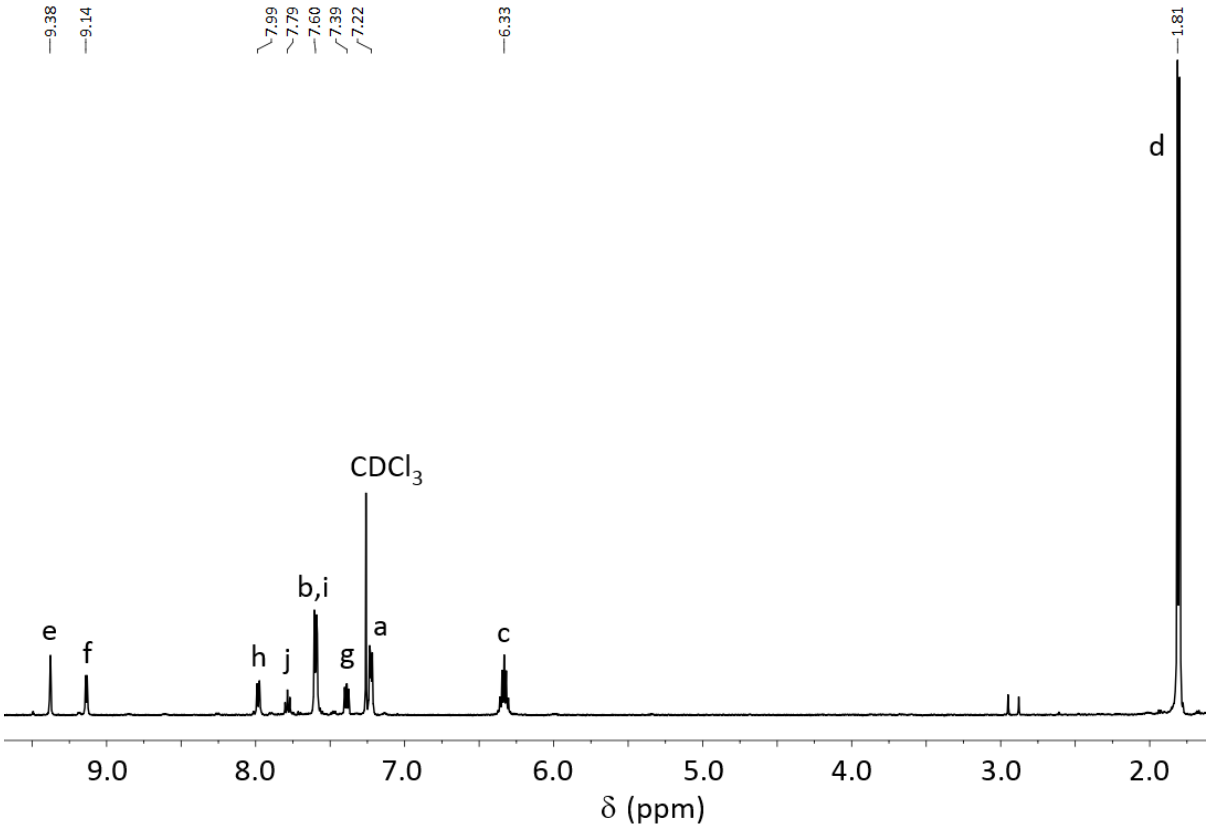

Figure 1.19 Partial ^{1}H NMR spectrum (298 K, 400 MHz, $CDCl_3$) of $[Pd_2(NHC)_2(\textbf{tripy})Br_4]$.

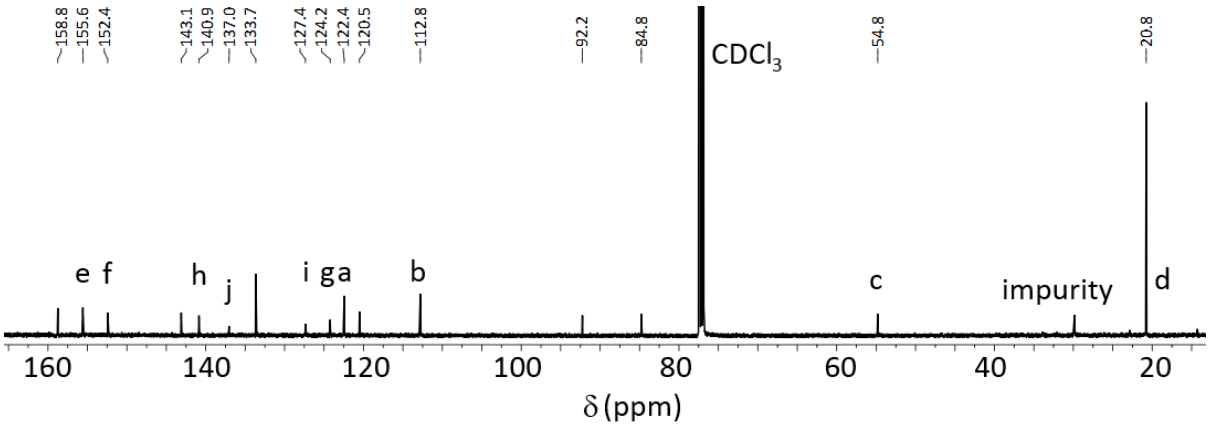

Figure 1.20 Partial ^{13}C NMR spectrum (298 K, 100 MHz, $CDCl_3$) of $[Pd_2(NHC)_2(\textbf{tripy})Br_4]$.

1.13 Attempted synthesis of $[Pd_2(NHC)_2(bntrz)Br_4]$

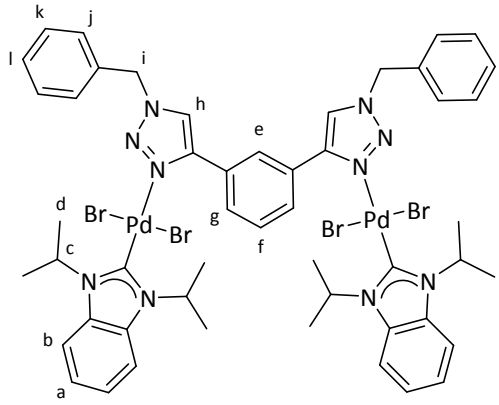

A solution of **bntrz** (8.38 mg, 0.021 mmol, 1 eq.) and dibromobis(benzimidazolin-2-ylidene)dipalladium(II)[3] (20 mg, 0.021 mmol, 1 eq.) in $CDCl_3$ (0.75 mL) was sonicated for 30 seconds. While X-Ray quality crystals of the complex could be obtained, ^{1}H-NMR showed a mixture of product, starting material, and a side product. Titrating in more of either of the reactants could not eliminate one of the unwanted species without increasing the amount of the other. In addition, some peaks were broadened, presumably due to hindered rotation between the *syn* and *anti* conformers, and altering the temperature did not resolve this. ^{1}H-NMR ($CDCl_3$, 298 K, 400 MHz) δ: (reporting only the peaks pertaining to the desired product within the reaction mixture) 8.85 (2H, br, H_g), 8.52 (1H, s, H_e), 7.90 (2H, s, H_h), 7.74 (1H, t, J = 8.7 Hz, H_f), 7.54 (4H, m, J = H_b), 7.35 -7.20 (>14H, m, H_j, H_k, H_l, H_a), 6.25 (4H, br, H_c), 5.61 (4H, br, H_i), 1.68 (24H, d, J = 3.6 Hz, H_d).

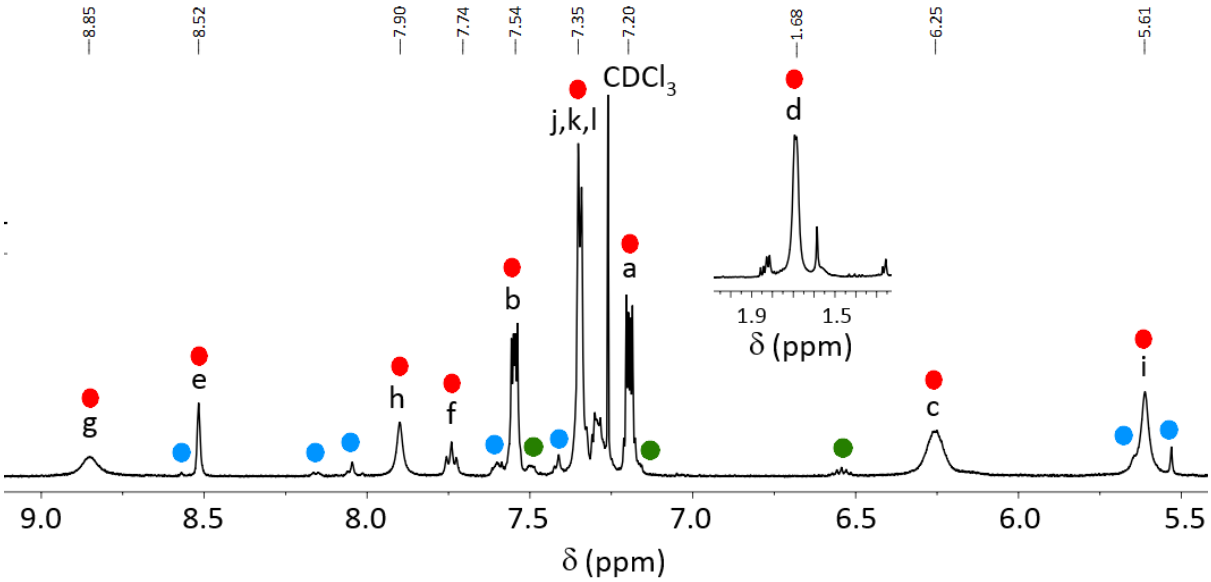

Figure 1.21 Partial ^{1}H NMR spectrum (298 K, 400 MHz, $CDCl_3$) of $[Pd_2(NHC)_2(\mathbf{bntrz})Br_4]$. Colour coding: ● disubstituted compound, ● dibromobis(benzimidazolin-2-ylidene)dipalladium(II) probe, ● side-product, most probably monosubstituted compound.

2 Cytotoxicity Studies

2.1 Methods

Reagents. MTT and cell culture reagents were purchased from Invitrogen (Auckland, NZ). Antibodies were purchased from Santa Cruz Biotechnology (CA, USA). All other chemicals were obtained from Sigma-Aldrich (Auckland, NZ) unless stated otherwise.

Cell Culture. All cell lines were purchased from the American Type Culture Collection (ATCC, Manassas, VA, USA) and maintained in Dulbecco's Modified Eagles Medium (DMEM) enriched with 2% FBS and 1% antibiotic. Additionally, the medium for MCF 10A cells was supplemented with 10 μg/mL insulin, 20 ng/mL EGF, 100 ng/mL cholera toxin and 0.5 μg/mL hydrocortisone. All cells were cultured at 37°C in a humidified atmosphere with 5% CO_2 levels.

Cytotoxicity Evaluation. Cell viability was assessed using the MTT (3-[4,5-dimethylthiazol-2-yl]-2,5-diphenyltetrazolium bromide) assay.[4] 96 well plates were seeded with 8,000 or 10,000 cells per well, and the cells left to adhere for 24 hours prior to treatment. Cells were then exposed to compound solubilized in DMSO. To control for the effects of DMSO, all cell culture medium had a constant DMSO concentration of 0.15 % (v/v). Following compound administration, cells were washed with PBS and MTT (0.4 mg⁄mL in DMEM) added for 3 hours. After MTT incubation, the medium was aspirated and the residual crystals dissolved in DMSO. Cell number was then calculated at λ = 550 nm.[4]

LDH Assay. LDH concentration was assumed to be proportional to the rate of oxidation of its substrate, NADH, under conditions of excess substrate.[5] Initially 40,000 cells were seeded into 24 well plates and left to adhere for 24 hours. The cells were then treated with helicate for the time indicated, and the extracellular media then collected and placed on ice. To measure media LDH activity, the media was combined with PBS, pyruvate (100 mM) and NADH (20 mM) and the change in absorbance at 340 nm (ε_{340} = 6,220 $M^{-1}cm^{-1}$) monitored.

Propidium Iodide and Hoechst 33342 Double Staining. A549 cells were seeded into 24 well plates at a density of 60,000 cells per well and left to adhere for 24 hours prior to treatment. Post treatment, the media was aspirated and replaced with Hoechst 33342 (2 μg/mL in DMEM) and incubated for 10 minutes. The cells were then washed with PBS and incubated with propidium iodide (50 μg/mL in DMEM) for a further 5 minutes. The cell monolayer was then washed with PBS (containing calcium and magnesium) and live cell imaging performed immediately using an inverted fluorescence microscope (Nikon Ti-U Eclipse, Coherent Scientific, Hilton, SA, Australia). Image analysis was performed using the ImageJ software package (National Institutes of Health, Bethesda, MD, USA).

Statistical Analysis. Statistical analyses and curve fitting were performed using OriginPro 8 (OriginLab Corporation, Northampton, MA). Statistical significance was accepted when $P<0.05$. Data was analysed with a one or two-way ANOVA combined with a Bonferroni post-hoc test. All data were expressed as means ± SEM unless otherwise stated.

3 Time Course ^{1}H NMR Stability Studies

All time course studies were carried out on a Varian 500 MHz VNMRS spectrometer at 298 K (3:2 d_6-DMSO/D_2O solvent mixture). The concentration of the Pd_2L_4 architectures was in all cases 2 mM. Testing was carried out against histidine, cysteine and tetramethylammonium chloride. In each cage 8 equivalents of the respective nucleophile was used. A reference sample of each dipalladium architecture at the correct concentration without nucleophile was used for time zero, with the exception of $[Pd_2(\mathbf{bntrz})_4](BF_4)_4$, which was not fully stable in DMSO. In this case, the reaction was set underway and the first spectrum run after 10 minutes. The amount of complex still present over time in comparison to at time zero was calculated through comparison of the integration of the peak found at highest chemical shift to the reference peak of trimethylsilyl propanoic acid, with additional comparison to the integration of peak belonging to the same proton in the free ligand in the cases where the free ligand was soluble in the solvent system used. This comparison to the amount of free ligand present was important in the case of $[Pd_2(\mathbf{bntrz})_4](BF_4)_4$ where free ligand was present from the outset of the experiment. The hexyl ligand, **hextrz** was not appreciably soluble in the solvent system used, but its cage was the most stable. Both **tripy** and **bntrz** had higher solubility, but after exceeding a given concentration and time both began to precipitate, but given this was beyond the halfway point of the reaction this did not influence measurement of the half-lives. The final ligand, **pegtrz**, was fully soluble in the solvent system used.

3.1 ^{1}H NMR Time Course Stackplots

3.1.1 Histidine

The introduction of histidine brought about the formation of two bis-histidine palladium(II) complexes, presumably diastereoisomers, and an accompanying downfield shift of the free histidine peaks. The half-lives of $[Pd_2(\mathbf{bntrz})_4](BF_4)_4$ and $[Pd_2(\mathbf{pegtrz})_4](BF_4)_4$ were reached at 12 hours, $[Pd_2(\mathbf{tripy})_4](BF_4)_4$ in 5 minutes, while a minimal amount (13%) of $[Pd_2(\mathbf{hextrz})_4](BF_4)_4$ was broken down.

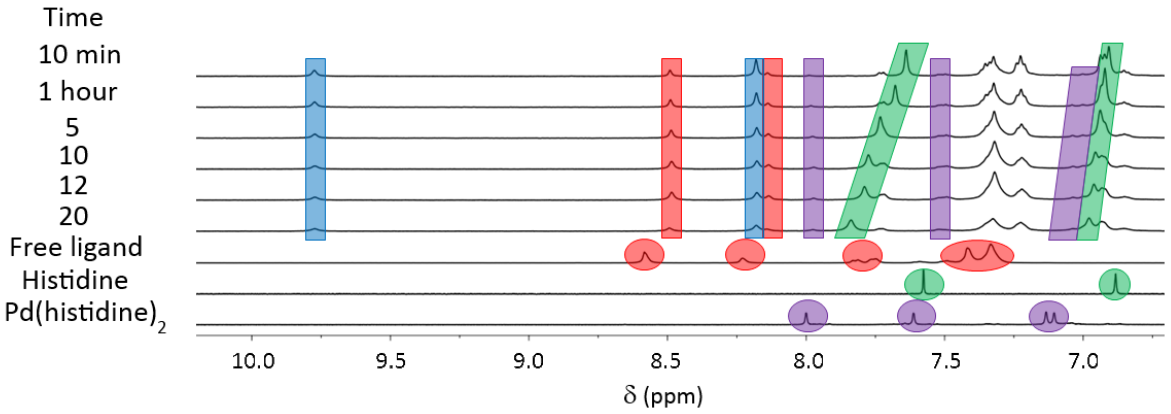

Figure 3.1 Time course partial ^{1}H NMR stackplot of $[Pd_2(\mathbf{bntrz})_4](BF_4)_4$ against 8 equivalents histidine (3:2 d_6-DMSO/D_2O, 298 K, 500 MHz). Colour coding: cage, free ligand, free histidine, $Pd(histidine)_2$ complexes.

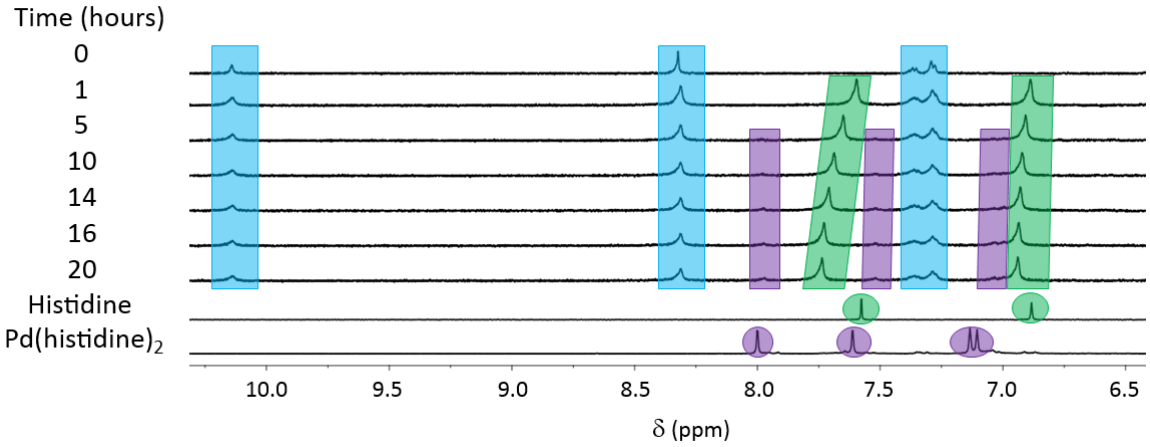

Figure 3.2 Time course partial ^{1}H NMR stackplot of $[Pd_2(\mathbf{hextrz})_4](BF_4)_4$ against 8 equivalents histidine (3:2 d_6-DMSO/D_2O, 298 K, 500 MHz). Colour coding: cage, free histidine, $Pd(histidine)_2$ complexes.

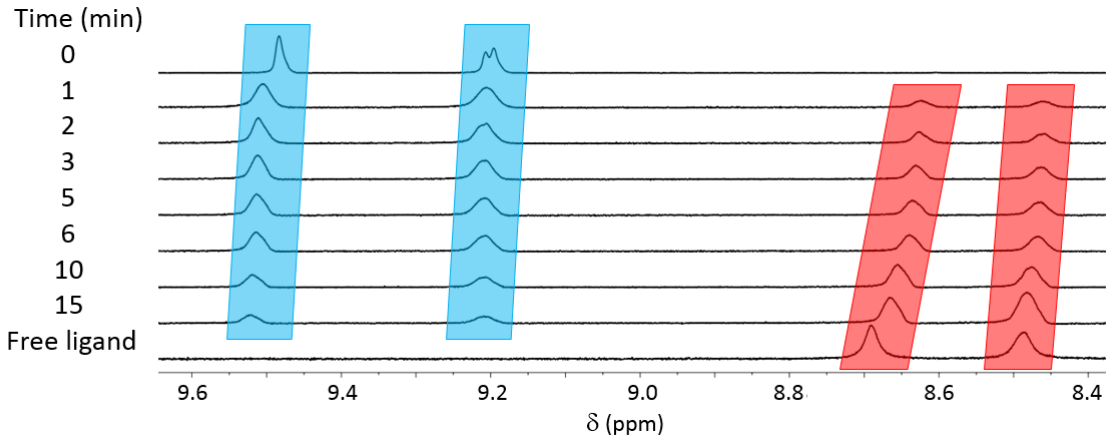

Figure 3.3 Time course partial ^{1}H NMR stackplot of $[Pd_2(\mathbf{tripy})_4](BF_4)_4$ against 8 equivalents histidine (3:2 d_6-DMSO/D_2O, 298 K, 500 MHz). Colour coding: cage, free ligand.

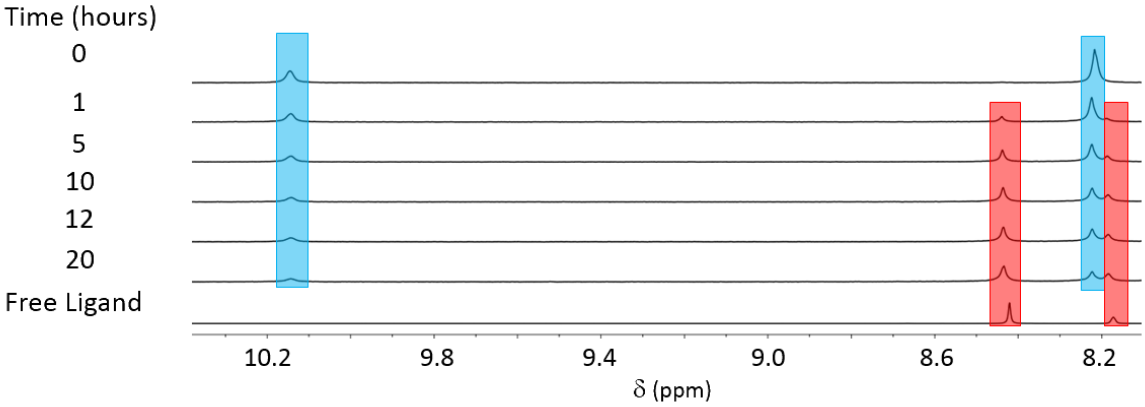

Figure 3.4 Time course partial ^{1}H NMR stackplot of $[Pd_2(\mathbf{pegtrz})_4](BF_4)_4$ against 8 equivalents histidine (3:2 d_6-DMSO/D_2O, 298 K, 500 MHz). Colour coding: cage, free ligand.

3.1.2 Cysteine

The only ^{1}H NMR peaks pertaining to the progressing reaction against this nucleophile in the aromatic region belonged to either cage or free ligand. The half-life $[Pd_2(\mathbf{bntrz})_4](BF_4)_4$ was reached in 30 minutes, $[Pd_2(\mathbf{pegtrz})_4](BF_4)_4$ in 20 minutes, $[Pd_2(\mathbf{tripy})_4](BF_4)_4$ in under one minute, while a minimal amount (13%) of $[Pd_2(\mathbf{hextrz})_4](BF_4)_4$ was broken down.

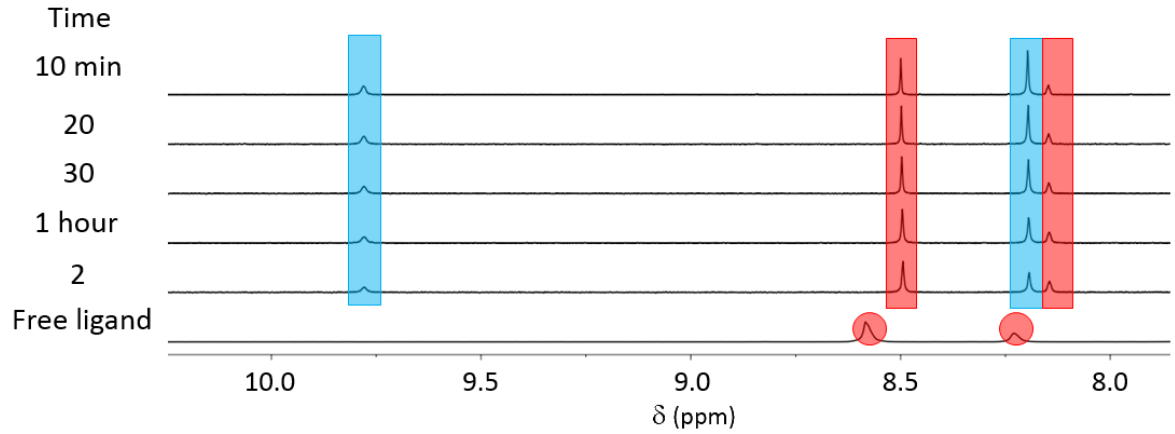

Figure 3.5 Time course partial ^{1}H NMR stackplot of $[Pd_2(\mathbf{bntrz})_4](BF_4)_4$ against 8 equivalents cysteine (3:2 d_6-DMSO/D_2O, 298 K, 500 MHz). Colour coding: cage, free ligand.

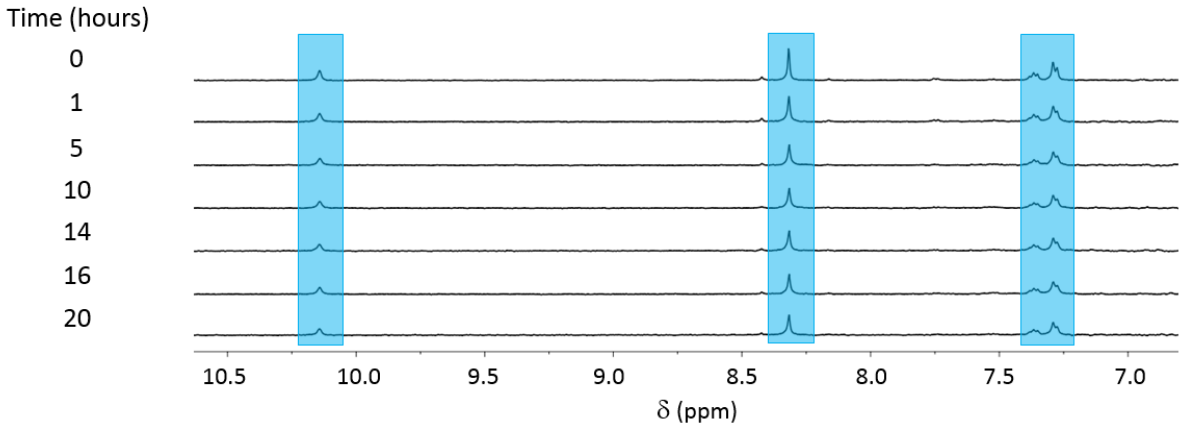

Figure 3.6 Time course partial ^{1}H NMR stackplot of $[Pd_2(\mathbf{hextrz})_4](BF_4)_4$ against 8 equivalents cysteine (3:2 d_6-DMSO/D_2O, 298 K, 500 MHz). Colour coding: cage.

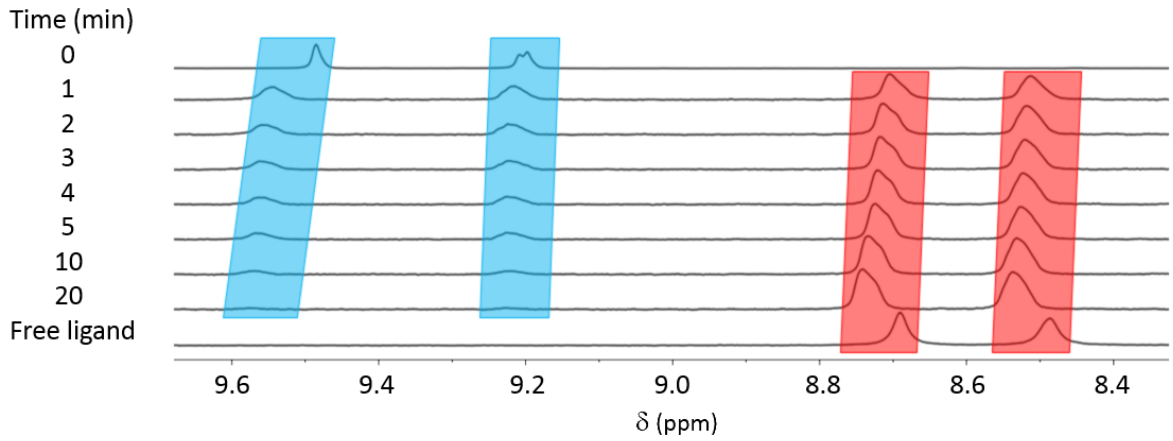

Figure 3.7 Time course partial ^{1}H NMR stackplot of $[Pd_2(\mathbf{tripy})_4](BF_4)_4$ against 8 equivalents cysteine (3:2 d_6-DMSO/D_2O, 298 K, 500 MHz). Colour coding: cage, free ligand.

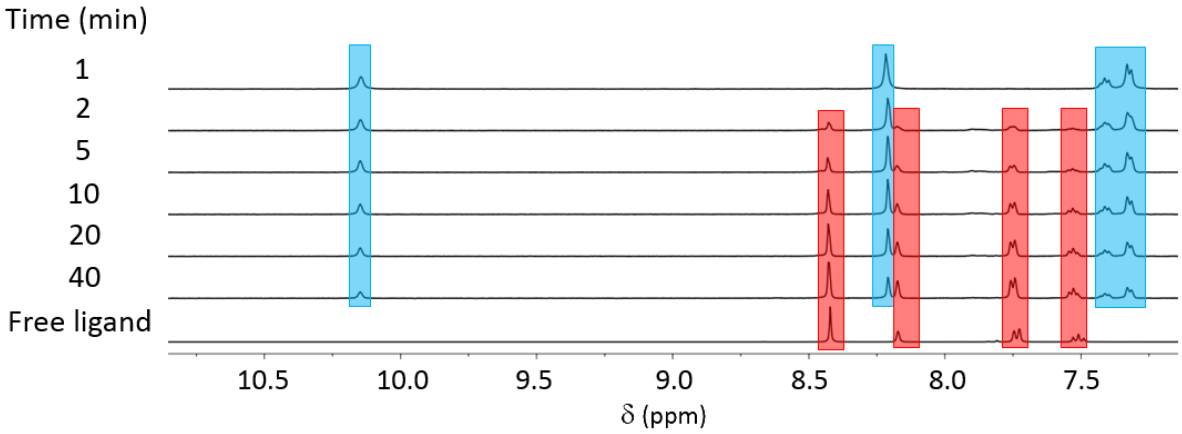

Figure 3.8 Time course partial ^{1}H NMR stackplot of $[Pd_2(\mathbf{pegtrz})_4](BF_4)_4$ against 8 equivalents cysteine (3:2 d_6-DMSO/D_2O, 298 K, 500 MHz). Colour coding: cage, free ligand.

3.1.3 Chloride

The only ^{1}H NMR peaks pertaining to the progressing reaction against this nucleophile in the aromatic region belonged to either cage or free ligand. In the case of $[Pd_2(\mathbf{tripy})_4](BF_4)_4$, introduction of tetramethylammonium chloride brought about a downfield shift of two proton resonances: those adjacent to the coordinating nitrogen of the cage, and in particular the proton directed towards the interior of the cage. This has previously been shown to be indicative of encapsulation of guest within the cavity, with the guest being either a halogen ion[6] or the chloride-containing cisplatin complex.[1c] As such it is likely that the downfield shift is due to encapsulation of the nucleophile, reinforced by the fact that no such shift occurs for the other, larger nucleophiles against $[Pd_2(\mathbf{tripy})_4](BF_4)_4$, and is furthermore not seen for chloride against the other three helicates, which do not have an internal cavity capable of guest encapsulation. The half-life $[Pd_2(\mathbf{tripy})_4](BF_4)_4$ was reached under a minutes, while negligible amounts of the triazole-based helicates were broken down.

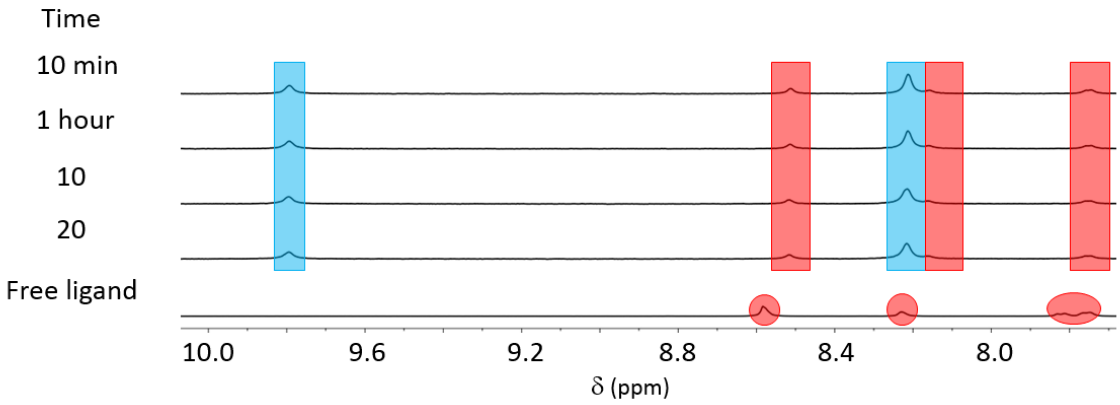

Figure 3.9 Time course partial ^{1}H NMR stackplot of $[Pd_2(\mathbf{bntrz})_4](BF_4)_4$ against 8 equivalents tetramethylammonium chloride (3:2 d_6-DMSO/D_2O, 298 K, 500 MHz). Colour coding: cage, free ligand.

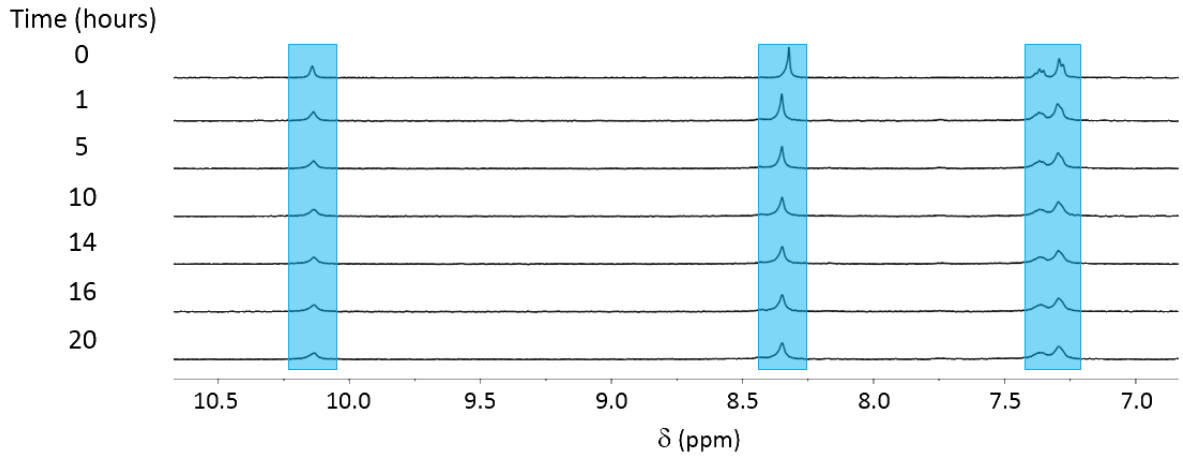

Figure 3.11 Time course partial ^{1}H NMR stackplot of $[Pd_2(\mathbf{hextrz})_4](BF_4)_4$ against 8 equivalents tetramethylammonium chloride (3:2 d_6-DMSO/D_2O, 298 K, 500 MHz). Colour coding: cage.

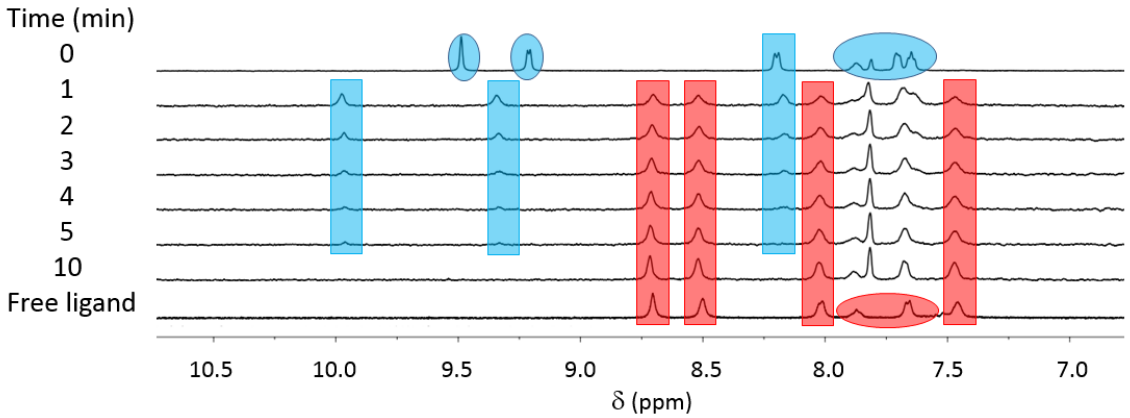

Figure 3.10 Time course partial ^{1}H NMR stackplot of $[Pd_2(\mathbf{tripy})_4](BF_4)_4$ against 8 equivalents chloride (3:2 d_6-DMSO/D_2O, 298 K, 500 MHz). Colour coding: cage, free ligand.

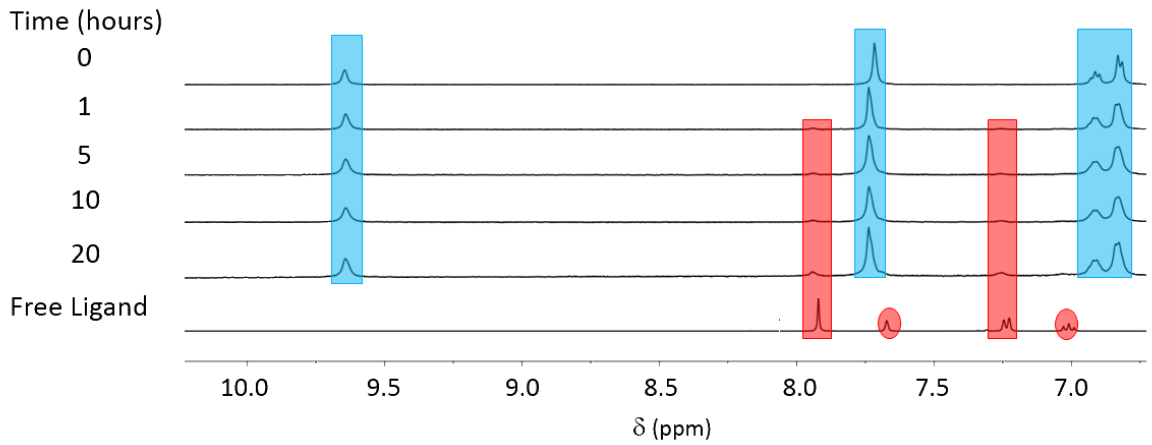

Figure 3.12 Time course partial ^{1}H NMR stackplot of $[Pd_2(\mathbf{pegtrz})_4](BF_4)_4$ against 8 equivalents chloride (3:2 d_6-DMSO/D_2O, 298 K, 500 MHz). Colour coding: cage, free ligand.

4 X-ray Data

4.1 Ethynylpyridyl probe

Orange block crystals were grown through vapour diffusion of diethyl ether into a solution of the complex in DCM. X-ray data were collected at 100 K on an Agilent Technologies Supernova system using Cu Kα radiation with exposures over 1.0°, and data were treated using CrisAlisPro[7] software. The structure was solved using X-Seed[8] and weighted full-matrix refinement on F^2 was carried out using SHELXL-97[9] running within the WinGX package[10]. All non-hydrogen atoms were refined anisotropically. Hydrogen atoms attached to carbons were placed in calculated positions and refined using a riding model. The structure was solved in the base monoclinic space group *C*2/*c* and refined to an R_1 of 2.31%. The asymmetric unit consists of one molecule of the complex.

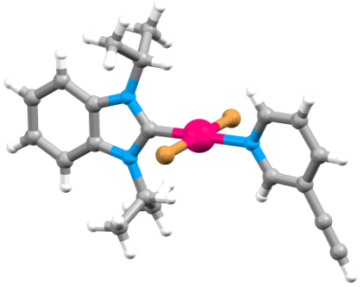

Figure 4.1 Mercury ball and stick representation of the asymmetric unit of [Pd(NHC)(ethynylpyridine)Br_2].

4.2 Benzyl probe

Yellow needle-like crystals were grown through vapour diffusion of diethyl ether into a solution of the complex in DCM and acetone. X-ray data were collected at 100 K on an Agilent Technologies Supernova system using Cu Kα radiation with exposures over 1.0°, and data were treated using CrisAlisPro[7] software. The structure was solved using X-Seed[8] and weighted full-matrix refinement on F^2 was carried out using SHELXL-97[9] running within the WinGX package.[10] All non-hydrogen atoms were refined anisotropically. Hydrogen atoms attached to carbons were placed in calculated positions and refined using a riding model. The structure was solved in the primitive orthorhombic space group $Pna2_1$ and refined to an R_1 of 3.26%. The asymmetric unit consists of a single molecule of the complex with one DCM molecule.

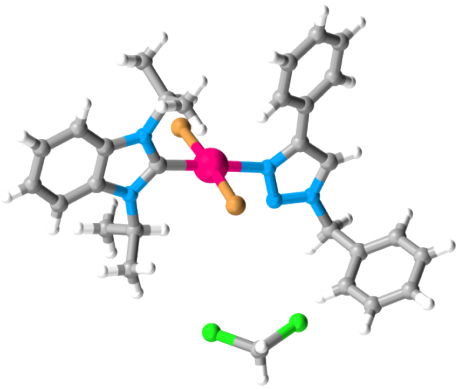

Figure 4.2 Mercury ball and stick representation of the asymmetric unit of [Pd(NHC)(**bntrz**)Br_2].·DCM.

4.3 PEG probe

Yellow needle-like crystals were grown through vapour diffusion of diethyl ether into deuterated chloroform. X-ray data were collected at 100 K on an Agilent Technologies Supernova system using Cu Kα radiation with exposures over 1.0°, and data were treated using CrisAlisPro[7] software. The structure was solved using X-Seed[8] and weighted full-matrix refinement on F^2 was carried out using SHELXL-97[9] running within the WinGX package[10]. Hydrogen atoms attached to carbons were placed in calculated positions and refined using a riding model. The structure was solved in the primitive orthorhombic space group $Pna2_1$ and refined to an R_1 of 3.47%. The asymmetric unit consists of a single molecule of the compound with no solvent molecules. The cif check on the structure returned a C alert for ambiguity in Flack test results (0.497 with standard uncertainty of 0.004). Solving the structure with inversion of total stereochemistry or solving as a twin gave worse test results with no improvement to R_1.

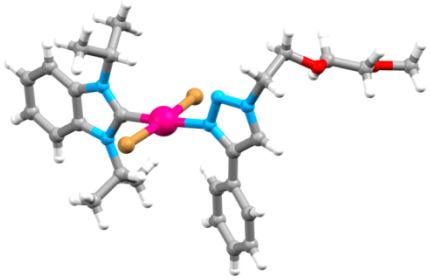

Figure 4.3 Mercury ball and stick representation of the asymmetric unit of [Pd(NHC)(**pegtrz**)Br_2].

4.4 Hexyl probe

Yellow needle-like crystals were grown through vapour diffusion of diethyl ether into deuterated chloroform. X-ray data were collected at 100 K on an Agilent Technologies Supernova system using Cu Kα radiation with exposures over 1.0°, and data were treated using CrisAlisPro[7] software. The structure was solved using X-Seed[8] and weighted full-matrix refinement on F^2 was carried out using SHELXL-97[9] running within the WinGX package[10]. Hydrogen atoms attached to carbons were placed in calculated positions and refined using a riding model. The structure was solved in the primitive orthorhombic space group $Pna2_1$ and refined to an R_1 of 2.68%. The asymmetric unit consists of a single molecule of the compound with no solvent molecules. Again, the cif check on the structure returned a C alert for ambiguity in Flack test results (0.485 with standard uncertainty of 0.007). Solving the structure with inversion of total stereochemistry or solving as a twin gave worse test results with no improvement in R_1.

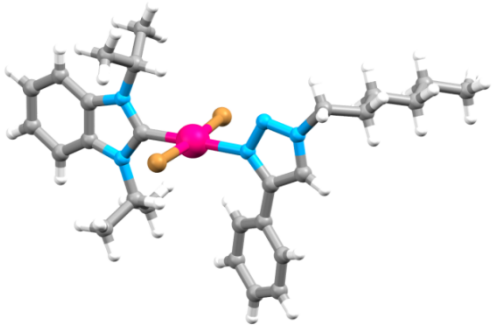

Figure 4.4 Mercury ball and stick representation of the asymmetric unit of [Pd(NHC)(**hextrz**)Br_2].

4.5 $[Pd_3(NHC)_2(tripy)Br_4]$

Slow evaporation of a chloroform solution of $[Pd_2(NHC)_2(tripy)Br_4]\cdot 4CHCl_3$. gave yellow crystals of $[Pd_3(NHC)_2(tripy)Br_4]\cdot 4CHCl_3$. X-ray data were collected at 100 K on an Agilent Technologies Supernova system using Cu Kα radiation with exposures over 1.0°, and data were treated using CrysAlisPro[7] software. The structure was solved using SIR-97[11] and weighted full-matrix refinement on F^2 was carried out using SHELXL-97[9] running within the WinGX[10] package. All non-hydrogen atoms were refined anisotropically. Hydrogen atoms attached to carbons were placed in calculated positions and refined using a riding model. The structure was solved in the triclinic space group $P\bar{1}$ and refined to an R_1 value of 11.0%. Present in the asymmetric unit is a $[Pd_3(NHC)_2(tripy)Br_4]$ complex and four solvent chloroform molecules. The chloroform molecules were slightly disordered and the ellipsoids of atoms C96 through C98 and Cl8 through Cl12 were slightly elongated when refined anisotropically. The ISOR command was employed to model these atoms. The carbon to chlorine distances in chloroform molecules were modelled with the DFIX command.

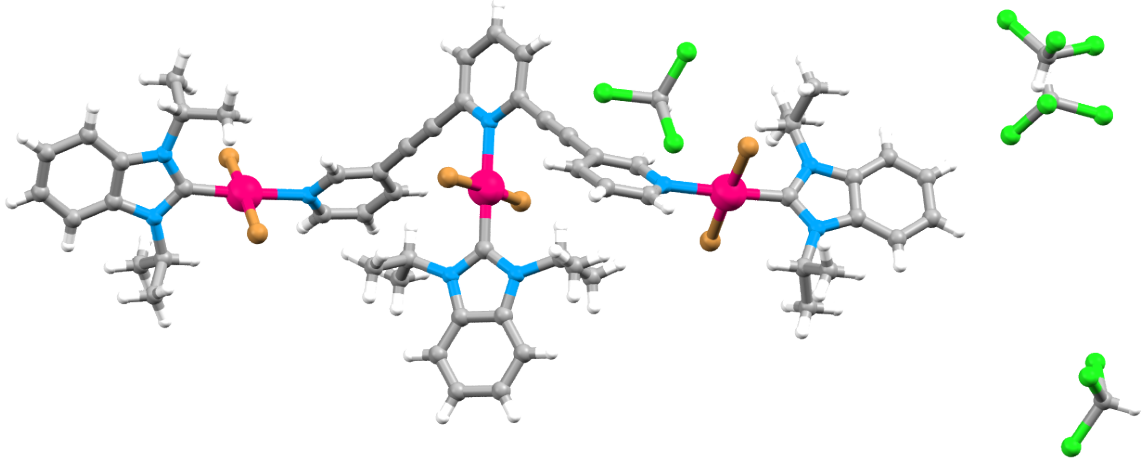

Figure 4.5 Mercury ball and stick representation of the asymmetric unit of $[Pd_2(NHC)_2(\mathbf{tripy})Br_4]\cdot 4CHCl_3$.

4.6 $[Pd_2(NHC)_2(bntrz)Br_4]$

Slow evaporation to dryness of a chloroform solution of the complex gave yellow crystals of $[Pd_2(\mathbf{bntrz})Br_4(NHC)_2]$. X-ray data were collected at 100 K on an Agilent Technologies Supernova system using Cu Kα radiation with exposures over 1.0°, and data were treated using CrysAlisPro[7] software. The structure was solved using SIR-97[11] and weighted full-matrix refinement on F^2 was carried out using SHELXL-97[9] running within the WinGX[10] package in conjunction with X-Seed.[8] All non-hydrogen atoms were refined anisotropically. Hydrogen atoms attached to carbons were placed in calculated positions and refined using a riding model. The structure was solved in the triclinic space group $P\bar{1}$ and refined to an R_1 value of 7.28%. Present in the asymmetric unit is a $[Pd_2(\mathbf{bntrz})Br_4(NHC)_2]$ complex.

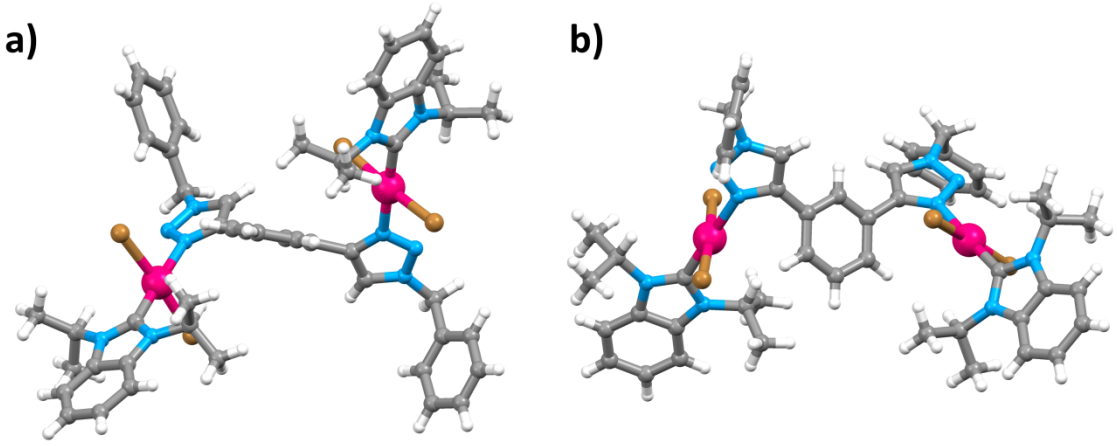

Figure 4.6 Mercury ball and stick representations **a)** from below and **b)** the side of the asymmetric unit of **X**, showing the *anti*-conformation adopted in solid state.

The crystal lattice contained diffuse electron density (within a solvent accessible void) that could not be appropriately modelled. The SQUEEZE routine within PLATON was employed to resolve this problem, resulting in void electrons count of 234 that we assign to four solvent chloroform molecules (232 electrons in total).

Table 4.1 SQUEEZE results for $[Pd_2(\mathbf{bntrz})Br_4(NHC)_2]$.

Platon squeeze void nr	1	2	3
Platon squeeze void average x	-0.003	0.402	0.597
Platon squeeze void average y	0.000	0.505	0.495
Platon squeeze void average z	0.000	0.713	0.287
Platon squeeze void volume	584	11	11
Platon squeeze void count electrons	230	2	2
Platon squeeze details	Electron density that could not be appropriately modelled, with the number of electrons consistent with four chloroform molecules.		

4.7 Data table

	ETHYNYL PYRIDINE	BENZYL	PEG	HEXYL
Empirical formula	$C_{20}H_{23}Br_2N_3Pd$	$C_{29}H_{33}Br_2Cl_2N_5Pd$	$C_{26}H_{35}Br_2N_5O_2Pd$	$C_{27}H_{37}Br_2N_5Pd$
Formula weight	571.63	788.72	715.81	697.84
Temperature	100.0(1) K	100.(2) K	100.0(1) K	100.0(1) K
Wavelength	1.54184 Å	1.54184 Å	1.54184 Å	1.54184 Å
Crystal system	Monoclinic	Orthorhombic	Orthorhombic	Orthorhombic
Space group	*C 2/c*	$Pna2_1$	$Pna2_1$	$Pna2_1$
Unit cell dimensions	a = 27.3117(2) Å α = 90° b = 9.98140(10) Å β = 96.5170(10)° c = 16.12290(10) Å γ = 90°	a = 8.9759(2) Å α = 90° b = 29.9396(6) Å β = 90° c = 11.4183(3) Å γ = 90°	a = 9.10290(10) Å α = 90° b = 30.3010(4) Å β = 90° c = 10.33980(10) Å γ = 90°	a = 8.90910(10) Å α = 90° b = 30.6079(4) Å β = 90° c = 10.68450(10) Å γ = 90°
Volume	4366.85(6) $Å^3$	3068.51(11) $Å^3$	2852.00(6) $Å^3$	2913.54(6) $Å^3$
Z	8	4	4	4
Absorption coefficient	11.199 mm^{-1}	9.747 mm^{-1}	8.784 mm^{-1}	8.528 mm^{-1}
F(000)	2240	1568	1432	1400
Theta range for data collection	3.26 to 74.20°	4.14 to 76.64°	4.52 to 76.74°	4.38 to 76.76°
Index ranges	-33<=h<=33, -12<=k<=12, -20<=l<=20	-11<=h<=8, -37<=k<=32, -14<=l<=11	-8<=h<=11, -37<=k<=37, -11<=l<=13	-11<=h<=10, -34<=k<=37, -13<=l<=8
Reflections collected	31042	12155	22580	16208
Independent reflections	4419 [$R_{(int)}$ = 0.0408]	5281 [$R_{(int)}$ = 0.0303]	5612 [$R_{(int)}$ = 0.0406]	4004 [$R_{(int)}$ = 0.0306]
Completeness	99.2 % to theta = 74.20°	99.2 % to theta =76.64°	99.2 % to theta = 76.74°	97.1 % to theta = 76.76°
Absorption correction	Gaussian	Gaussian	Gaussian	Gaussian
Refinement method	Full-matrix least-squares on F^2	Full-matrix least-squares on F^2	Full-matrix least-squares on F^2	Full-matrix least-squares on F^2
Data / restraints / parameters	4419 / 6 / 239	5281 / 1 / 356	5612 / 1 / 330	4004 / 1 / 321
Goodness-of-fit on F^2	1.122	1.102	1.052	1.025
Final R indices [I>2sigma(I)]	R1 = 0.0231, wR2 = 0.0587	R1 = 0.0326, wR2 = 0.0796	R_1 = 0.0347, wR_2 = 0.0874	R_1 = 0.0268, wR_2 = 0.0702
R indices (all data)	R1 = 0.0233, wR2 = 0.0600	R1 = 0.0341, wR2 = 0.0805	R_1 = 0.0360, wR_2 = 0.0880	R_1 = 0.0276, wR_2 = 0.0708
Absolute structure parameter	-	-0.011(10)	0.488(9)	0.241(8)
Largest diff. peak and hole	0.662 and -0.545 e.$Å^{-3}$	0.740 and -0.723 .Å-3	0.678 and -0.545 e.Å-3	0.584 and -0.690 e.Å-3

	TRIPYRIDYL PROBE	BENZYL TRIAZOLE
Empirical formula	$C_{62}H_{69}Br_6Cl_{12}N_9Pd_3$	$C_{50}H_{56}Br_4N_{10}Pd_2$
Formula weight	2164.32	1329.49
Temperature	100.0(1) K	100.(2) K
Wavelength	1.54184 Å	1.54184 Å
Crystal system	Triclinic	Triclinic
Space group	P-1	P-1
Unit cell dimensions	a = 9.3316(3) Å α = 72.281(2)° b = 16.9562(5) Å β = 80.109(2)° c = 25.8379(5) Å γ = 88.820(3)°	a = 12.2308(5) Å α = 75.175(2)° b = 12.6784(4) Å β = 85.812(3)° c = 20.4542(5) Å γ = 81.398(3)°
Volume	3834.27(18) $Å^3$	3029.69(17) $Å^3$
Z	2	2
Absorption coefficient	13.481 mm^{-1}	8.177 mm^{-1}
F(000)	2112	1316
Theta range for data collection	3.72 to 76.75°	3.64 to 74.98°
Index ranges	-11<=h<=11, -20<=k<=21, -25<=l<=32	-13<=h<=15, -15<=k<=15, -25<=l<=24
Reflections collected	62918	44918
Independent reflections	16012 [$R_{(int)}$ = 0.1009]	12182 [$R_{(int)}$ = 0.0745]
Completeness	100.0 % to theta = 67.00°	97.5 % to theta = 74.98°
Absorption correction	Semi-empirical from equivalents	Semi-empirical from equivalents
Refinement method	Full-matrix least-squares on F2	Full-matrix least-squares on F2
Data / restraints / parameters	16012 / 57 / 841	12182 / 0 / 603
Goodness-of-fit on F^2	1.235	1.538
Final R indices [I>2sigma(I)]	R_1 = 0.1103 wR_2 = 0.3006	R_1 = 0.0728 wR_2 = 0.2181
R indices (all data)	R_1 = 0.1382 wR_2 = 0.3333	R_1 = 0.0863 wR_2 = 0.2308
Absolute structure parameter	-	-
Largest diff. peak and hole	6.796 and -2.458 e.$Å^{-3}$	4.332 and -2.078 e.$Å^{-3}$

5 References

[1] a)J. D. Crowley, E. L. Gavey, *Dalton Trans.* **2010**, *39*, 4035; b)S. O. Scott, E. L. Gavey, S. J. Lind, K. C. Gordon, J. D. Crowley, *Dalton Trans.* **2011**, *40*, 12117; c)J. E. M. Lewis, E. L. Gavey, S. A. Cameron, J. D. Crowley, *Chem. Sci.* **2012**, *3*, 778.

[2] V. Gudipati, D. P. Curran, C. S. Wilcox, *J. Org. Chem.* **2006**, *71*, 3599.

[3] H. V. Huynh, Y. Han, R. Jothibasu, J. A. Yang, *Organometallics* **2009**, *28*, 5395.

[4] T. Mosmann, *J Immunol Methods* **1983**, *65*, 55.

[5] H. U. Bergmeyer, E. D. Bernt, *Methods of Enzymatic Analysis* **1974**, *2*, 636.

[6] S. Freye, J. Hey, A. Torras-Galan, D. Stalke, R. Herbst-Irmer, M. John, G. H. Clever, *Angew. Chem., Int. Ed.* **2012**, *51*, 2191.

[7] O. CrysAlisPro; Agilent Technologies: Yarnton, England, 2012.

[8] L. J. Barbour, *J. Supramol. Chem.* **2001**, *1*, 189.

[9] G. Sheldrick, *Acta Cryst.* **2008**, *A64*, 112.

[10] L. Farrugia, *J. Appl. Cryst.* **1999**, *32*, 837.

[11] A. Altomare, M. C. Burla, M. Camalli, G. L. Cascarano, C. Giacovazzo, A. Guagliardi, A. G. G. Moliterni, G. Polidori, R. Spagna, *J. Appl. Cryst.* **1999**, *32*, 115.